APPLICATION OF FLOW-THROUGH SOLID-PHASE-SYNTHESIS TO THE FLUORESCENT LABELING OF AMINES WITH CARBOXYLIC ACID FUNCTIONALIZED BODIPY DYES

William Owen Doerksen

A master's thesis submitted in partial fulfillment

of the requirements for the degree of

Master's of Science in Chemistry

DATE: September 10th, 2024

ABSTRACT

The use of fluorophores for the labelling of biomolecules in living cells has become a key method for understanding processes in cellular biology. Synthetic fluorescent molecules can be introduced non-specifically to uniformly stain cells or selectively label a protein of interest to visualize cellular activity and metabolism using fluorescent microscopy. An increasingly popular small molecule fluorophore at the forefront of fluorescent cellular observation is the group known as the 4,4-difluoro-4-bora-3a,4a-diaza-*s*-indacene (BODIPY) dyes. This particular family of fluorophores are known to be strongly UV-absorbing and emit sharp fluorescent peaks with high quantum yields. Characteristics that make BODIPY dyes even more desirable for biological imaging are their insensitivity to the polarity and pH of their environment allowing them to stay reasonably stable at physiological conditions. Structural modifications to the BODIPY core allow for the fine tuning of its photochemical properties and allow a certain level of fluorescence control – however these changes can result in long, often low-yielding syntheses. As part of this research, a solid-phase-synthesis (SPS) method was developed as a flow through system to efficiently attach a variety of BODIPY fluorophores to amine-functionalized compounds. In order for this reaction to occur, the fluorophore requires a carboxylic acid moiety available to attach to the resin and subsequently couple to an amine through amide bond linkage. The synthesis of these BODIPY derivatives will also be described.

This work demonstrates an efficient method for coupling different BODIPY dyes to a variety of amines as well as the preparation of an AMPS-DCT resin used for amide coupling using SPS. The resulting fluorescent compounds will be tested for fluorescent characteristics to provide further insight into the effects that structural modification has on the fluorophore's attractive photochemical properties.

ACKNOWLEDGEMENTS

I would like to express my deepest gratitude to my supervisor, Dr. Campbell, for his unwavering support, guidance, and encouragement throughout the course of my graduate studies. His expertise, patience, and insightful feedback have been invaluable in shaping this thesis and my growth as a researcher.

I extend my sincere thanks to the members of my committee, Dr. Gottardo and Dr. Jiang, as well as the faculty of the department of chemistry at Lakehead for providing a stimulating and collaborative environment that has greatly contributed to my academic and personal development. My experience has been unique and rewarding and I’m fortunate to have completed this work at such an esteemed school surrounded by brilliant minds.

Thank you all for making this journey possible.

TABLE OF CONTENTS

LIST OF FIGURES

LIST OF TABLES

Page

LIST OF ABBREVIATIONS

AMPS	Aminomethyl polystyrene
BODIPY	4,4-Difluoro-4-bora-3a,4a-diaza-*s*-indacene
DCT	Dichlorotriazine
FRET	Fluorescence resonance energy transfer
NMM	*N*-methylmorpholine
PET	Photoinduced electron transfer
SPS	Solid phase synthesis
UV	Ultraviolet

1. INTRODUCTION

1.1. Fluorescent Probes and Their Utility in Research

The mechanism of fluorescence occurs in a two-step chemical process where a specific molecule absorbs light in the form of photons at a particular wavelength and re-emits it at a higher wavelength. How efficient a molecule absorbs and emits light depends on the properties of said molecule, termed fluorophores or fluorescent probes. If a fluorophore is able to convert a large portion of the absorbed light into emitted light, it has a high quantum yield due to its high ratio of the number of photons emitted to the number of photons absorbed. Initially, the absorption of high-energy photons by electrons promotes a singlet in the ground state to a singlet in the excited state. The resulting excited state is short-lived, so in order for the electrons to return to ground state they first undergo vibrational relaxation and then release lower energy photons which causes fluorescence and can be detected at a higher wavelength.

Due to the unique nature of the fluorescent mechanism, fluorophores are widely used in drug discovery, cellular imaging, environmental analysis, and various medical applications. Specifically, small-molecule fluorescent probes are particularly sought after for these applications because their fluorescent emissions can be measured with great sensitivity and allow for high spatial and temporal resolution during fluorescence microscopy cell imaging.[1] The first small-molecule fluorophore to be discovered was the natural product quinine, an

important molecule for both medicinal and organic chemistry.[2] In 1845 the visible emission from an aqueous quinine solution was reported, shortly followed by characterization of its fluorescent spectra by George Gabriel Stokes; Stokes Shift, is the term used to describe the difference in wavelength between absorption and emission maximums (Figure 1).

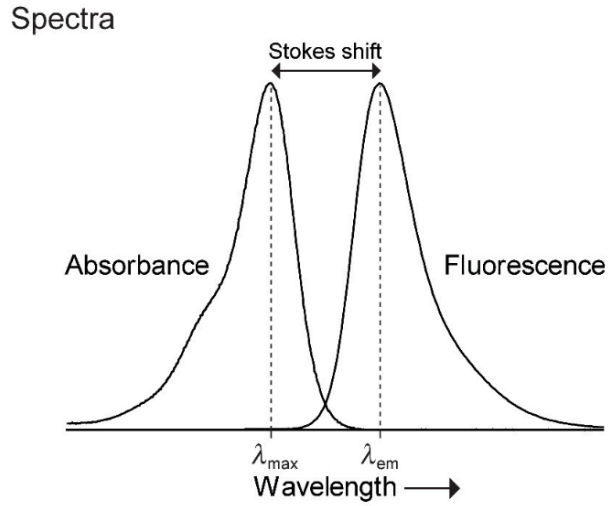

Figure 1. Stokes shift.

Quinine is a member of a class of fluorophores known as endogenous fluorophores, consisting of many naturally occurring fluorescent compounds. Among these are common aromatic amino acids such as phenylalanine and tyrosine, which each exhibit weak fluorescence under UV light. The most fluorescent natural amino acid is tryptophan with a λ_{max} of 280 nm, λ_{em} of 348 nm, and a quantum yield of 0.13 (Figure 2).[3] Tryptophan fluorescence has been advantageous as an index for signaling a variety of biological processes such as protein folding and ligand binding, as well as being used in fluorescence

resonance energy transfer (FRET) applications.[4] Reduced nicotinamide cofactors such as NADH also exhibit measurable fluorescence with $\lambda_{max}/\lambda_{em}$ of 340/435 nm, however, endogenous compounds that exhibit the most significant fluorescence signals are flavin mononucleotides with $\lambda_{max}/\lambda_{em}$ 450/530 nm and a quantum yield of 0.25 (Figure 2).[4,5] The collective fluorescence of endogenous fluorophores in biological samples can give rise to a phenomenon known as "autofluorescence", which is the natural emission of light by biological structures and can render desirable signals obscured and unintelligible from labelled targets.

A more common class of compounds, that encompasses a larger variety of applications, are polycyclic aromatic fluorophores, with notable members of this class being the naphthalene derivatives. The compound 5-((2-aminoethyl)amino)naphthalene-1-sulfonic acid (EDANS) has remained widely used since its discovery in 1973 as a donor for FRET-based nucleic acid probes and protease substrates (Figure 2).[6] As a fluorescent probe, small-molecule fluorophores such as EDANS acid are able to change their fluorescence emission in response to a binding event, chemical reaction, or alteration to their immediate environment. For this to be useful, however, the fluorophore needs to show specificity to its target, which can pose a challenge synthetically while developing derivatives and can also have an effect on their spectral properties.

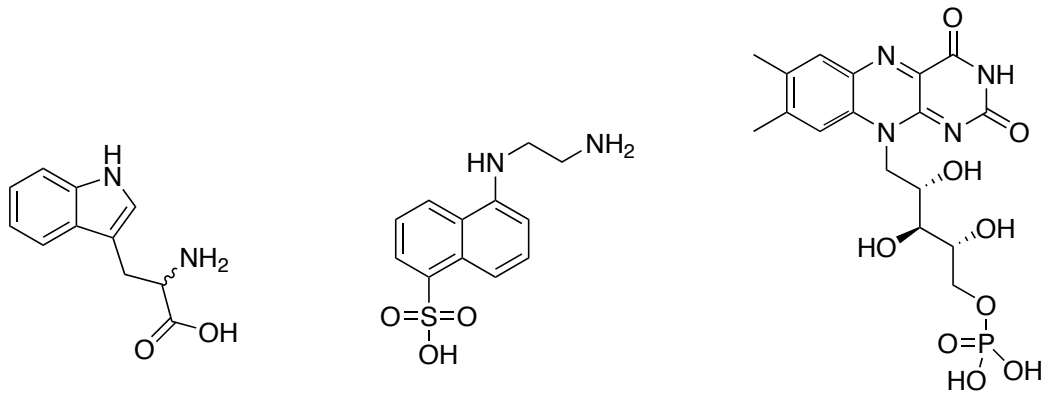

Tryptophan EDANS Flavin Mononucleotide

Figure 2. Structures of common fluorescent molecules.

Perhaps the most utilized fluorophore in history - remaining widely used since it was first synthesized in 1871 – is the extremely versatile fluorescent dye known as fluorescein. Although it belongs in the same polycyclic aromatic fluorophore class as EDANS, when comparing their photochemical characteristics, fluorescein is unmatched in both quantum yield (0.95 for fluorescein, vs. ~0.27 for derivatives of EDANS) and extinction coefficient (9.3 x 10^4 $M^{-1}cm^{-1}$ for fluorescein, vs. 5.4 x 10^3 $M^{-1}cm^{-1}$ for EDANS), which is a characteristic of how efficiently a molecule absorbs light.[6,7] Like EDANS, fluorescein is also acidic in nature and contains a benzoic acid substituent attached to a tricyclic xanthene structural motif. Fluorescein (Figure 3) takes its monoanion form around pK_a *5* and dianion form upon deprotonation around pK_a 6.35, with the latter being its most fluorescent form and displaying a fluorescent profile with $\lambda_{max}/\lambda_{em}$ 490/514 nm. Possibly fluorescein's most notable role is its therapeutic application in iris fluorescein angiography, for which it serves as a

vital indicator for elucidating a wide range of eye pathologies.[8] More recently fluorescein derivatives have found use in pretargeting approaches for recognition of tumor-associated antigens which can be visualized *in vivo* due to their synthetically derived near-infrared photochemical properties.[9]

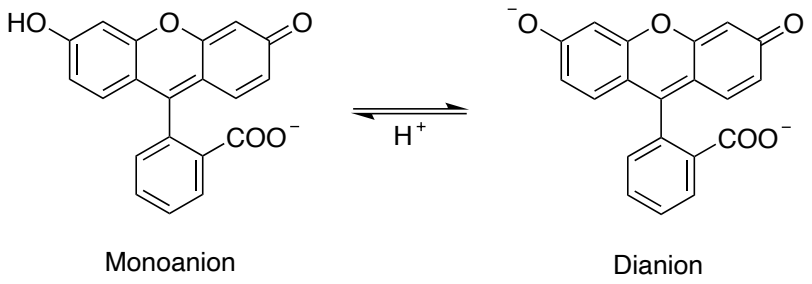

Figure 3. Deprotonated fluorescein forms.

Visualizing metabolic processes *in vivo* using fluorescent tags continues to gain traction in research as previous limits of visualization methods are overcome. Specifically, improving diffraction limits involving fluorescence microscopy techniques has produced a number of high-resolution methods that allow for the detection of individual molecules as well as their exact location. Methods such as photoactivated localization microscopy (PALM) and single-particle-tracking PALM (sptPALM) rely on the labelling of target proteins with fluorophores that are capable of photoactivation.[10] Such methods, which use fluorescently tagged proteins, rely on the basic principle that the fluorescent tag does not inhibit any cellular or physiological processes involving the protein, and can be tracked as well as visualized using high-resolution fluorescence microscopy. For example, the use of confocal microscopy – a high-resolution

fluorescence microscopy technique – has successfully established the localization of natural killer T cells during their initial response to activation using fluorescently labelled target proteins in mouse models *in vivo*.[11]

Until recently, it has not been possible to gain sufficient fluorescence microscopy spatial resolution beyond about 200 nm despite cellular structures of interest existing on the nanoscale (10nm – 100nm) in biological samples. As mentioned previously, researchers have been finding ways to overcome diffraction limits, as well as resolution difficulties, that often rely on new and improved high-resolution fluorescence microscopy methods. A common feature of these new approaches is to use fluorophores that have the ability to fluorescently switch “on” or stay “off” depending on what state the fluorophore is in during sample observation. For example, stimulated emission depletion (STED) microscopy relies on fluorescent switching being induced at defined coordinates with subdiffraction resolution (resolution beyond the diffraction limit), allowing for the localization of single molecular labels in biological samples.[12] In contrast, single molecule localization microscopy (SMLM) allows switching to occur at random and emission of the fluorophore is measured within a diffraction-limited area; the sample size is predetermined and is often used as a localization confirmation method with respect to the biomolecule that is fluorescently tagged.[13]

As diffraction and resolution limits in fluorescence microscopy are overcome, the pursuit of innovative fluorophores serving specific visualization purposes in

research continues to generate complicated structure modifications. This can pose as a threat in the new fluorescent frontier as increasingly complicated syntheses are needed to satisfy structural requirements that have been modified from existing scaffolds. Similarly, strategic structural modifications on existing fluorophores may result in difficult syntheses when exploring the fluorescent labelling of biomolecules. Therefore, the presence of functional groups on fluorophores capable of conjugation is important for the labelling of biomolecules. For example, the previously mentioned fluorescein fluorophore contains a carboxylic acid group that is capable of undergoing active ester synthesis, which involves the reaction of the carboxylic acid group undergoing activation with a coupling agent such as N-hydrosuccinimide (NHS) and 1-ethyl-3-(3-dimethylaminopropyl) carbodiimide (EDC) and forming an amide bond with an amino group on a biomolecule.[14] For biomolecules containing available cysteine residues, fluorescein can be functionalized with maleimide groups that allow for maleimide-thiol coupling to take place. Click chemistry has also been employed for reactions involving fluorescein fluorophores containing azide groups and are specific to biomolecules modified with alkyne groups, which received Nobel Prize recognition in 2022. These reactions are normally catalyzed by copper(I) ion containing groups and form triazole linkage between the biomolecule and fluorescein, allowing for bioorthogonal reaction outcomes.[14] For example, a newly designed, readily-available fluorescent copper-chelating

azide has been prepared by combining a small bicyclic azaphthalimide dye with

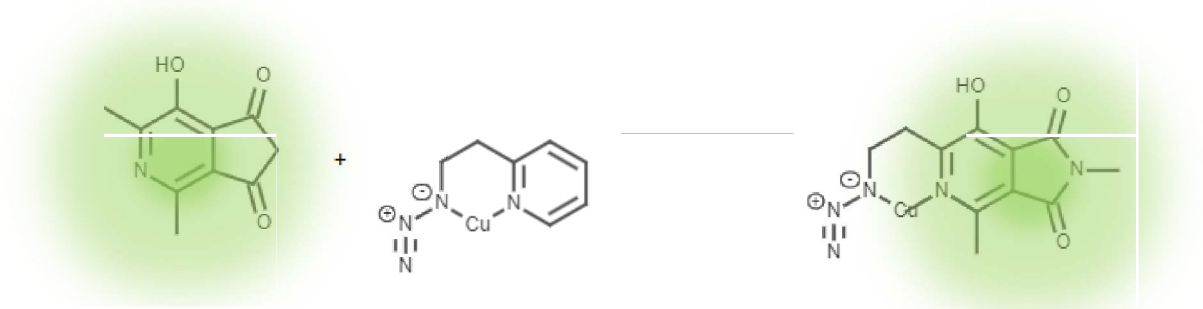

Figure 4. Fluorescent copper-chelating azide.

The versatility of fluorescein as a widely used bioconjugation fluorophore has resulted in some notable characteristic developments, but it also has limitations for its use in research. As mentioned previously, fluorescein has a pKa of 6.35 which makes it pH-sensitive; it is susceptible to changes in its fluorescent intensity and spectral properties depending on the pH of its environment. As with most fluorophores, fluorescein is also susceptible to photobleaching during prolonged exposure to light, resulting in destruction of its ability to fluoresce. Most notably, fluorescein is prone to hydrolysis which can pose a significant issue when being used in long-term experiments with biological samples.[15] An innovative group of fluorophores now being used as labelling alternatives to fluorescein and other fluorescent molecules is the family of molecules known as BODIPY dyes.

1.2. BODIPY Dyes

BODIPY dyes, short for BOron-DIPYrromethene dyes, were originally discovered in the late 1960s by a research group led by Professor Michael C. Whiting during their investigation into new and improved synthetic dyes. By 1968, the structure of the BODIPY core (4,4-difluoro-4-bora-3a,4a-diaza-*s*-indacene) had been elucidated with the simplest derivative containing methyl groups attached to the alpha positions of the core which act to increase quantum yield (Figure 5).[16] It was immediately noted upon investigation that the synthesized BODIPY fluorophore exhibited intense fluorescence and high photostability, two important characteristics for potential biological and spectroscopic applications. Their discovery laid the foundation for development and exploration into this new family of fluorescent dyes.

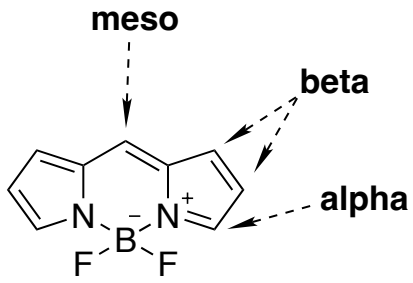

Figure 5. BODIPY (4,4-difluoro-4-bora-3a,4a-diaza-s-indacene) "core" position designation.

Structural investigations into the BODIPY core have allowed for diversification at the meso, beta, and alpha positions. It was soon discovered that attachment of substituents around the core had an effect on photochemical properties such as absorption and emission, quantum yield, and photostability,

specifically at the alpha and beta positions.[16] This stabilization can occur through the introduction of electron-donating or electron-withdrawing groups which can have an effect on the electronic structure of the fluorophore, leading to a disparate distribution of electron density and therefore affecting the energy levels of the molecular orbitals involved in absorption and emission processes.[17] Essentially, the addition of electron-donating groups increases the electron density of the BODIPY core causing a red-shifted emission spectrum, while electron-withdrawing groups decrease the electron density and can shift the emission spectra to a lower wavelength, known as a blue-shifted spectrum. These processes are possible in BODIPY fluorophores due to a process known as photoinduced electron transfer (PeT).

PeT is a fundamental process that is able to occur between a donor moiety and an acceptor moiety. Upon photoexcitation from incoming light, an electron is transferred to the acceptor moiety from the donor moiety which has a lower electron affinity. The efficiency of this process is dependent on specific electronic properties and the spatial arrangement of the donor and acceptor moieties, as well as the energy level alignment between both substituents. BODIPY dyes that undergo PeT tend to see a decrease in fluorescence intensity as a result – known as fluorescence quenching – due to the disruption of the radiative decay pathway of the excited BODIPY molecule by means of electron transfer.[17]

PeT in BODIPY fluorophores can be strategically employed as a detection method for sensing the presence of analytes or specific environmental conditions; specific donor and acceptor moieties can be incorporated into BODIPY molecules which interact with analytes that encourages PeT to take place.[18] The resulting fluorescence quenching that occurs is able to be detected, allowing for the design of sensitive and selective BODIPY-based sensors which turn “off” in the presence of targeted analytes for quantification. For example, the detection of the hypochlorite anions (ClO^-) in biological samples has been made possible by taking advantage of its affinity for a specific BODIPY fluorophore functionalized with a substituted benzene moiety (Figure 6).[19,52] The reaction between the benzene moiety and hypochlorite ions in solution led to a significant change in the fluorescence emission of the fluorophore, leading to the successful imaging of endogenous hypochlorite in living cells with significant sensitivity.

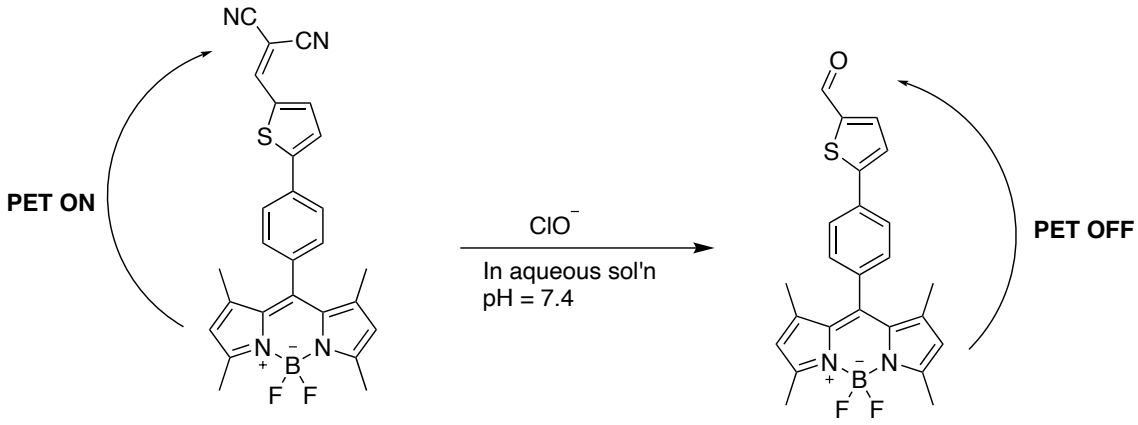

Figure 6. Hypochlorite sensing in cells via functionalized BODIPY derivative.

Although their use as sensors has provided innovative methods for analyte and reactive oxygen species detection in biological samples, BODIPY fluorophores are versatile enough to also be employed as probes, being directly attached to biomolecules of interest or even synthesized for the purposes of localization studies and fluorescence microscopy detection. Recently, the use of BODIPY probes to target and observe the mitochondria of eukaryotic cells has become increasingly popular to provide useful information on organelle morphology.[22,23,24] These studies tend to focus on the utilization of delocalized lipophilic cations in order to compensate the negative mitochondrial membrane potential, with the most popular mitochondria-targeted delivery moiety being triphenylphosphonium (TPP^+).[20] In one study, researchers were able to incorporate TPP^+ and triethylamine (TEA^+) into two novel BODIPY probes through a short, efficient synthesis for the purpose of guiding the fluorophore into the mitochondrion (Figure 7).[21] BODIPY was able to maintain its superior photochemical properties as well as pH stability and photostability upon entrance into the organelle, thus providing a new technique for live-cell imaging with low cytotoxicity.

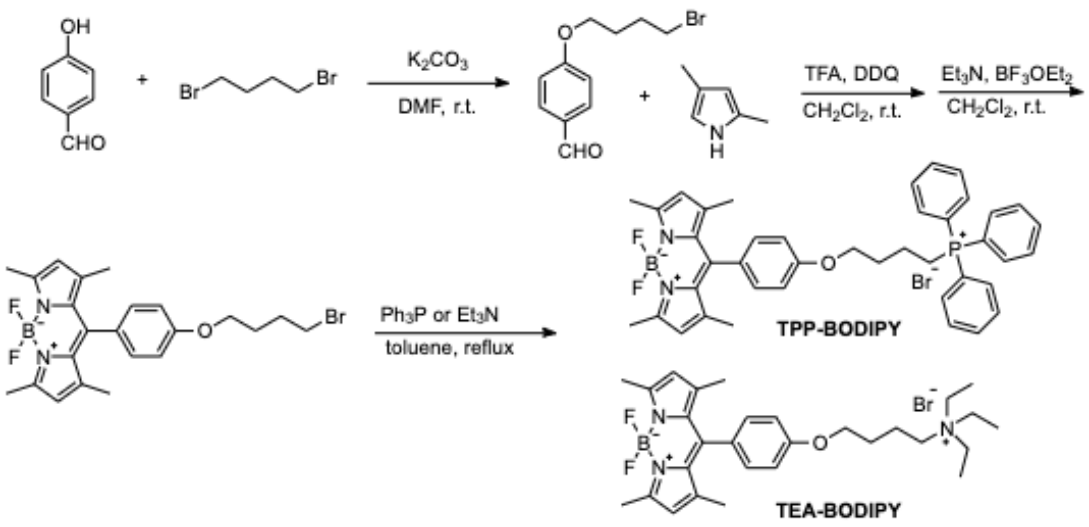

Figure 7. BODIPY synthesis resulting in TPP and TEA derivatives.

Although targeting the mitochondria of cells using BODIPY probes is becoming increasingly popular, newly developed probes are finding their place in a wide variety of intracellular visualization studies. One such study was developed with the purpose of developing a highly reliable fluorescent probe for the selective imaging of tau neurofibrillary tangles which have long been associated with Alzheimer's disease progression.[25] A short synthesis was conducted after molecular docking investigations that combined the commercially available asymmetric BODIPY core with a functionalized benzaldehyde, and it was found that the new BODIPY fluorophore (BT1) showed high selectivity to tau neurofibrillary tangles confirmed by immunofluorescence analysis detection (Figure 8).[26]

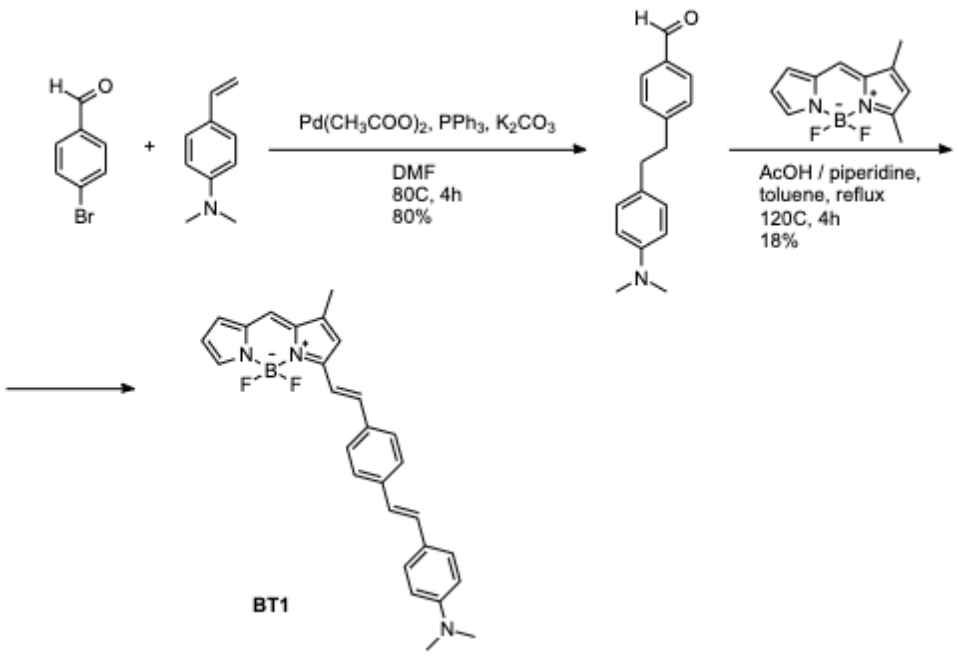

Figure 8. Synthesis of highly selective BODIPY fluorophore BT1.

1.3. BODIPY Syntheses

Fine-tuning of photochemical properties of BODIPY dyes can be accomplished by characterizing certain parts of the fluorophore through specific synthesis. The most common synthetic route to the BODIPY core involves the acid catalyzed condensation of an aromatic aldehyde **2** with pyrrole **1** which affords the dipyrromethane intermediate **3**, an unstable compound sensitive to light and air.[16] Oxidation results in the formation of dipyrrin **4**, which can finally be subjected to a base – usually triethylamine (Et_3N) - and boron trifluoride diethyl etherate ($BF_3{\cdot}OEt_2$) to yield a BODIPY core **5** with an aromatic substituent in the *meso* position (Figure 9).

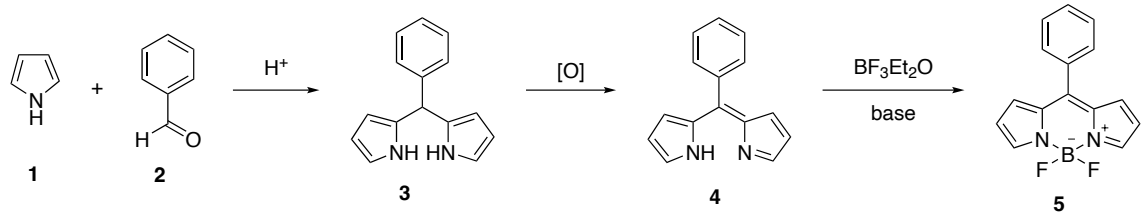

Figure 9. Common aromatic-aldehyde BODIPY synthetic route.

There are also synthetic routes to yield non-aromatic substituents in the *meso* position of the core; a similar method as mentioned above involves an acid catalyzed condensation of an acylpyrrole, **8**, with pyrrole moiety, **1**. This method first requires a condensation reaction with pyrrole **1** and an acylium equivalent, **6**, to produce asymmetric dipyrrins, **9**, using almost the exact same acidic reaction conditions as previously mentioned. This specific method can be employed using an acid chloride, anhydride, or an orthoester, and the resulting compound is the BODIPY core **10** functionalized with an R group at the *meso* position (Figure 10).[27] This synthetic approach can be expanded further to yield more substituted BODIPY dyes depending on the pyrrole used in the condensation. For example, by using 2,4-dimethylpyrrole in place of pyrrole **7** in the acid catalyzed step, the resulting BODIPY core will contain α,β-substituted methyl groups that have been shown to increase overall quantum yields due to the occurrence of PeT.[16]

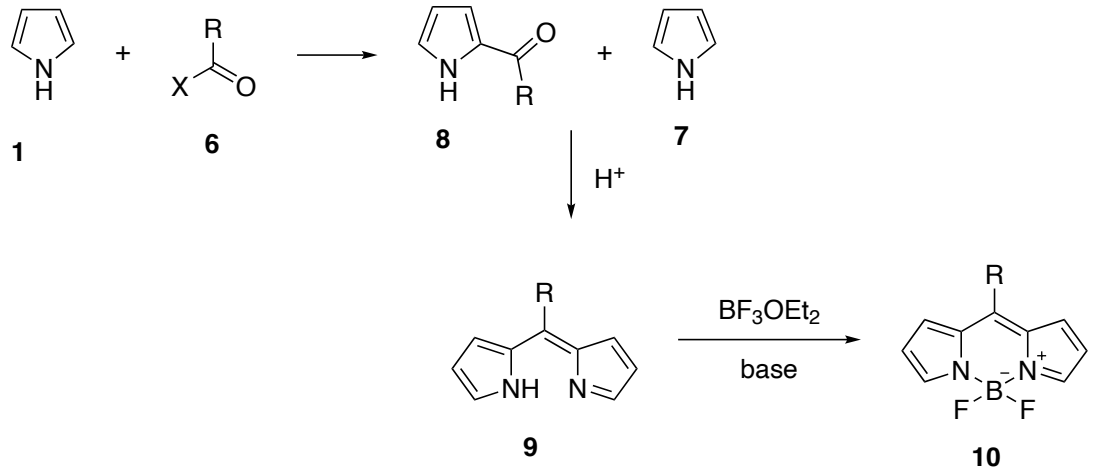

Figure 10. Acylpyrrole synthesis method; X = Cl, Br, OOCR.

The use of acid anhydrides in BODIPY synthesis is useful in that new compounds are able to be functionalized directly with carboxylic acid moieties, important handles for selective conjugation and modification. Carboxylic acids can react with primary amines on biomolecules such as amino acids and proteins to form stable amide bonds in what's known as peptide bond formation in bioconjugation.[28] Compounds containing carboxy groups can also undergo esterification reactions when they react with alcohols to form ester linkages, allowing for another method of bioconjugation. One specific reaction scheme reported by Li and colleagues[27] was successful in constructing an α,β-methylated BODIPY core that contained a butanoic acid moiety in the *meso* position. Their synthesis was a relatively simple and efficient one-pot reaction beginning with 2,4-dimethylpyrrole **11** reacting with glutaric anhydride **12** in the presence of a small amount of coordinating agent $BF_3{\cdot}OEt_2$ (Figure 11). The

crude mixture was then subjected to similar conditions as previously mentioned (Et_3N; $BF_3{\cdot}OEt_2$) to produce a butanoic functionalized BODIPY dye **13**, in 16% yield, capable of undergoing esterification with cholesterol analogues.

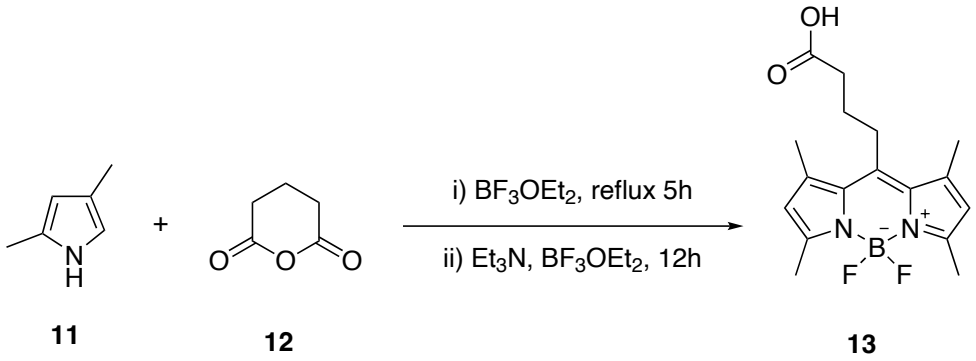

Figure 11. One-pot carboxylic acid-BODIPY synthesis.

A more recent investigation by Wang et al. was able to take advantage of some commercially available acid anhydrides to produce two new carboxylic acid functionalized BODIPY dyes.[29] Specifically, they used similar reaction conditions and were able to distinguish their carboxy moiety based on their starting acid anhydride; succinic anhydride **14** produced a propanoic moiety in the *meso* position while phthalic anhydride **15** yielded a benzoic acid moiety (Figure 12). The respective yields of the functionalized BODIPY analogues were 21% for compound **16** and 25% for compound **17**, and it is worth noting that increased reaction time of the initial refluxing step is believed to have an effect on the overall yield of the reaction.[16,29,30] These specific BODIPY analogues were synthesized using pyrrole and 2,4-dimethylpyrrole to investigate the effects of core methylation on photochemical properties – it was found that the methyl

groups increased the fluorescence quantum yields (up to 0.80 in water) but negatively affected the photostability of the dyes, and the unsubstituted analogues performed better in photooxidation and photodegradation experiments. Photodegradation studies focus on the chemical damage of fluorescent species which is enhanced by prolonged illumination. This causes photoinduced damage through the cycling of photon absorption and emission, so the rates of fluorophore photobleaching can be observed depending on the physical properties of the fluorophore. The use of dry solvents as well as molecular sieves (4 Å) is essential to maintain anhydrous conditions throughout the reaction due to the production of water as more dye is produced.

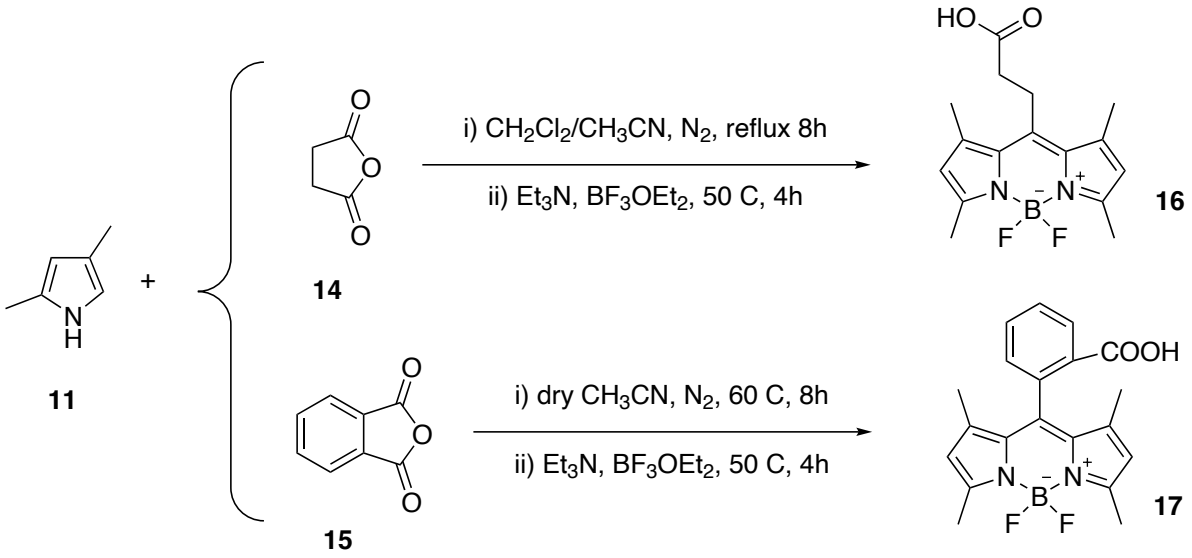

Figure 12. Butanoic and benzoic acid functionalized BODIPY dyes.

The convenient synthesis of a substituted pyrrole with acid anhydrides results in higher yields compared to the longer syntheses with aldehydes and acyl halides and allows for the release of a free carboxyl group directly during

the formation of the BODIPY framework. The coupling of this carboxylic moiety to a *N*-hydroxysuccinimide (NHS) ester is now one of the most common methods for conjugating the dye to a protein, antibody, and other types of biomolecules.[31] A specific method to achieve the esters of dyes by NHS is via the *N,N'*-disuccinimidyl carbonate **18** reaction with an unmethylated dye **19** in the presence of excess triethylamine (Figure 13).[29] This reaction has been shown to be successful in synthesizing an activated BODIPY dye-NHS ester **20** for the purposes of fluorescence labeling of BSA and was observed by the naked eye at levels as low as 2 ng.

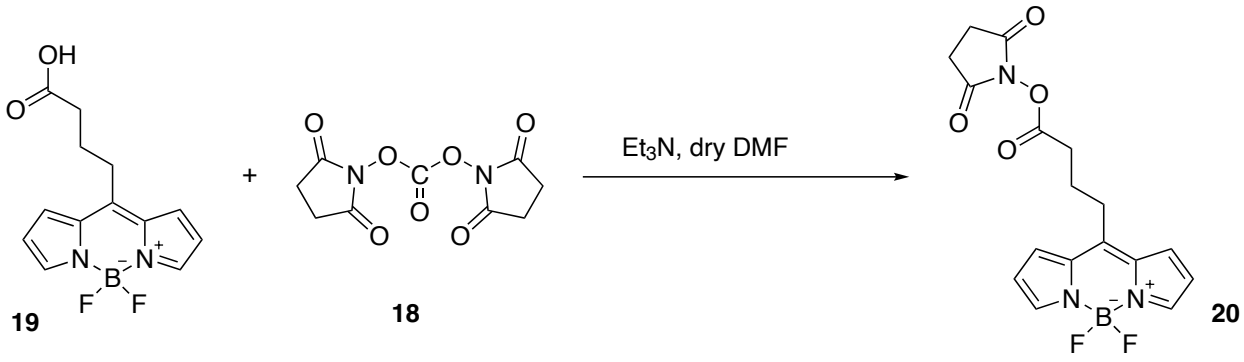

Figure 13. Carboxyl functionalized BODIPY dye with NHS-ester linkage.

The mechanism through which an activated NHS ester reacts with a biomolecule occurs through nucleophilic attack, usually where a primary amine ($-NH_2$) acts as a nucleophile and attacks the carbonyl carbon of the ester. The release of an *N*-hydroxysuccinimide results in a newly formed amide bond covalently linking the biomolecule to the carboxylic acid. This type of conjugation reaction is widely used due to its efficiency and selectivity when labeling primary

amines such as lysine as well as its mild reaction conditions that help prevent side reactions with thiols and hydroxy groups.[33] However, optimization of reaction parameters such as pH and reaction time can drastically influence outcomes and is essential for optimal conjugation. For example, NHS esters are typically more reactive at slightly alkaline pH (pH 7-9). They are also prone to hydrolysis in aqueous solutions and can degrade over time, limiting shelf life and affecting their reliability and consistency for conjugation

Although activated NHS esters are commonly used, there are some obvious drawbacks to their practicality as conjugation reagents. The syntheses of BODIPY dyes containing the essential carboxyl moiety are relatively low yielding, with the highest reported yielding 25%.[27,29] As the final product is then used for bioconjugation, it is important that as much product be produced in the shortest number of steps possible. These considerations leave opportunities for new methods of fluorophore conjugation to biomolecules. A possible novel route for the conjugation of BODIPY fluorophores is the use of flow-through solid-phase-synthesis (SPS) that is capable of directly attaching a functionalized BODIPY fluorophore to a biomolecule, eliminating the need for any NHS-ester activation, isolation and subsequent bioconjugation.

1.4. Application of Flow-Through Solid-Phase-Synthesis with BODIPY Fluorophores

Recent development of SPS techniques have showcased how sophisticated and convenient chemical synthesis can be when approaching them strategically.[49,50] Compounds synthesized on solid supports are able to be released without the tethered linkers that are used in intermediate steps, allowing only the target molecule to be collected with most of the by-products of the reaction remaining on the solid support or prior elution. Thus, high product purity is often a characteristic of SPS without the need for additional purification steps. Simplified purification is a key advantage over traditional synthesis which often involves laborious purification techniques such as column chromatography. Perhaps where SPS holds the most potential over traditional synthesis is in its efficiency. By immobilizing reactants on a solid support, the effective molar concentrations of reagents are significantly higher compared to traditional solution chemistry (Figure 14). This allows for increased reaction efficiency and faster reaction kinetics.[35,36]

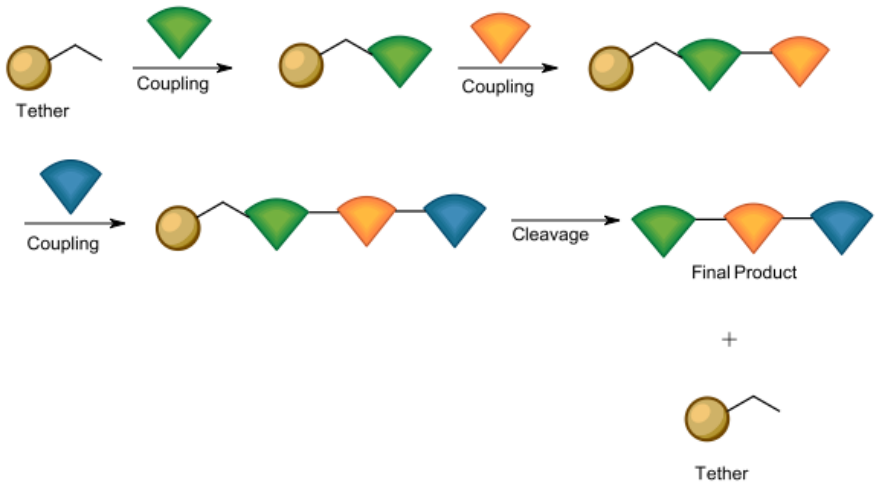

Figure 14. General SPS coupling scheme illustrating the consecutive addition and tethering of reactants.

In industry, the advantageous characteristics of SPS have been exploited to expand its capabilities in automated customized synthesis. This is a result of advances in end-to-end continuous-flow synthesis that have merged with SPS, allowing for improvements in scalability and reproducibility. For example, an automated multistep synthesis of prexasertib was able to produce the small-molecule pharmacophore in 65% isolated yield, and also established 23 novel prexasertib derivatives.[37] The minimized interactions between individual synthetic steps permitted the multistep scheme to be applied with a variety of functional groups and also enabled diversification of derivatives at early stages as well as late. Oftentimes SPS is applied in the production of long peptide chains and proteins using standard coupling techniques in what's known as solid-phase peptide synthesis (SPPS).[38]

The original SPPS method used by Merrifield[39] displayed a growing peptide chain anchored to the solid support through the C-terminal carboxyl while elongation occurred from the N-terminal. However, since then, , a more generalized methodology has been shown to allow amino acid side chains and C- and N-termini to be exposed by anchoring the molecule through a backbone amide linker (BAL). This method has been proven to be efficient for attachment to the solid – most often polymeric – support, and is an essential first step which requires maximum linkage stability to the subsequent chemical transformations.[41] The most common method for products to be released from the polymeric support are under acidic conditions that result in C-N bond cleavage – these supports are usually designed from substituted benzyl[42], benzhydryl[43], and trityl[44] derivatives and are especially sensitive to treatment with trifluoroacetic acid (TFA).[40]

In order for SPS reaction kinetics to be assessed, new real-time monitoring techniques are constantly being employed that allow the study of reaction progression and efficiency. Specifically, the attachment of fluorescent probes onto solid supports allows the immobilization of the probe in close proximity to the reaction site and any changes or transformations occurring during synthesis can therefore be monitored based on changes in fluorescence properties. The fluorophores in question would be designed to exhibit changes in excitation and emission upon certain synthetic events such as coupling, deprotection, and purification and allow for optimization of reaction conditions.

For example, the proteolysis of peptides immobilized on microarray surfaces is now able to be monitored for site specificity and efficiency of the protease using fluorescent amino acids.[45]

In some cases, fluorophores can be attached directly to the target molecule being synthesized during SPS, and if the changes in fluorescence properties are intense enough, this allows for direct monitoring of the target molecule formation. In one study, a solid support resin was preloaded with a BODIPY propanoic fluorophore and prepared multiple triterpenoid-BODIPY conjugates using a novel, fast, and simple SPS method. The resin used was an aminomethyl polystyrene (AMPS) solid support equipped with a BAL, and the subsequent steps resulted in the BODIPY fluorophore being linked to the resin and cleaved through acylation of the AMPS-BAL resin.[46] AMPS resins possess primary amine groups which are essential for coupling reactions and are highly stable under typical SPS reaction conditions. The high loading capacity, swelling properties, and Fmoc (9-fluorenylmethoxycarbonyl) protection compatibility are all characteristics that make AMPS resins a popular choice for SPS.[47]

The goal of this study is to develop an easy and efficient method for attaching fluorescent BODIPY probes onto biomolecules which utilizes a flow-through SPS on an AMPS resin. Specifically, three BODIPY derivatives will be functionalized with carboxylic acid moieties that should be able to couple to amines and form an amide bond linkage. A specialized AMPS-DCT (dichlorotriazine) resin (Figure 15) and coupling procedure will be described, and

subsequent photochemical data of successful BODIPY derivatives will be interpreted that will provide insight into the effects amide coupling has on fluorescence characteristics of the BODIPY core.

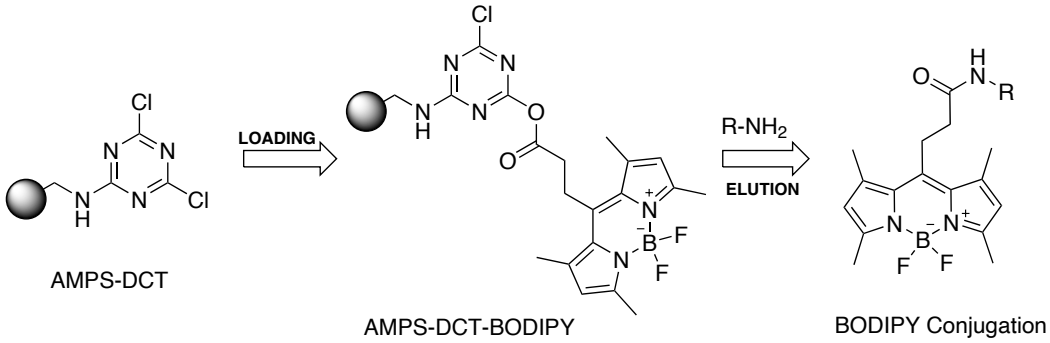

Figure 15. AMPS-DCT overall coupling scheme.

2. RESULTS

2.1. Synthesis of Carboxylic Acid Functionalized BODIPY Dyes

The development of a novel method for SPS of fluorescent probes began with synthesizing BODIPY dyes that are able to undergo amide coupling. Three BODIPY dye derivatives were synthesized with propanoic **16**, butanoic **13**, and benzoic acid **17** substituents in the *meso* position of the core. The syntheses combined the findings of previous studies[27,29,30], starting with an initial reaction between the substituted 2,4-dimethylpyrrole **11** and succinic **14**, glutaric **12**, or phthalic anhydride **15**, in the presence of coordination agent $BF_3{\cdot}OEt_2$ (Figure 16). The reaction time was extended for this step in the synthesis from 5 hours to 18 hours in an effort to improve overall yield, after which Et_3N was added along with additional $BF_3{\cdot}OEt_2$ and reacted for a further 12 hours. Compounds **16** and **13** were synthesized in 22% and 20% yields, respectively, while compound **17** was synthesized in 27% yield. A substituted pyrrole was chosen for the scaffold of the BODIPY derivative due to the electron donating effect methyl groups exhibit on the core and overall quantum yield increase in the final products.[27]

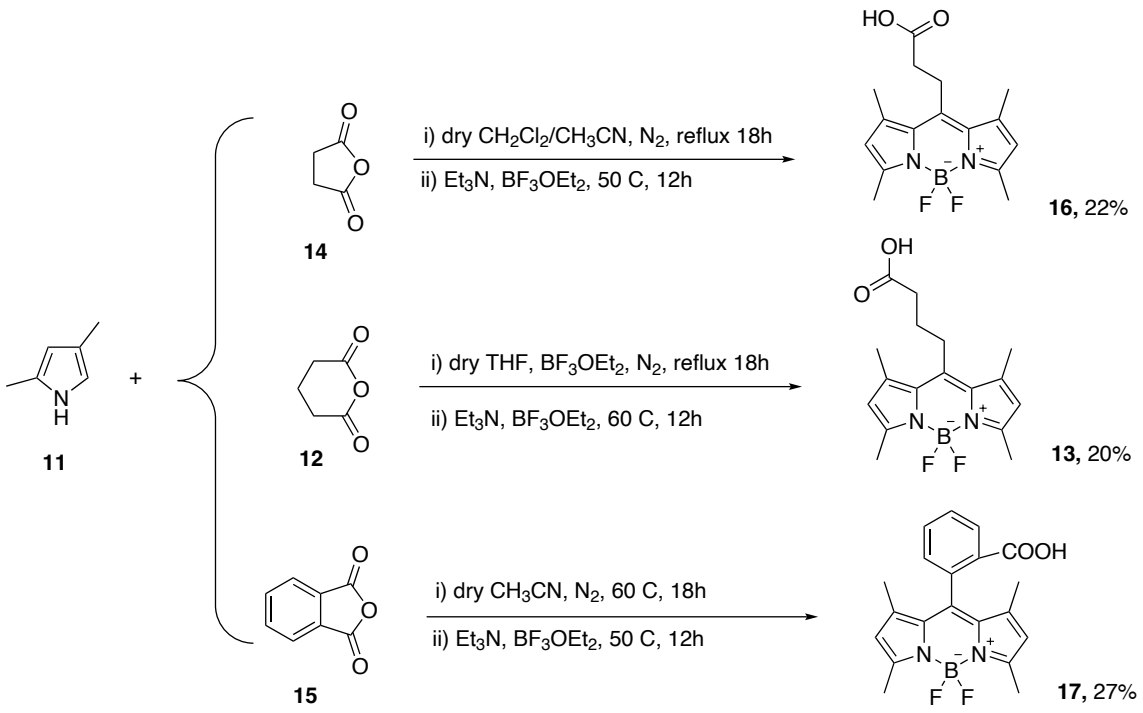

Figure 16. Carboxylic acid functionalization reaction scheme of previously reported structures.

2.2. Amide Coupling of Carboxy Functionalized BODIPY Dyes via AMPS-DCT Resin

A DCT functionalized resin was synthesized starting with commercially available AMPS resin. Approximately 100-150 mg of AMPS resin can be added to the propylene filter tube that is attached to a syringe which is then saturated with solvent. This was followed by addition of cyanuric chloride that's dissolved in 20 mL of solvent and then flowed through via the syringe to ensure saturation of the resin - the resulting solid support is now an AMPS-DCT resin ready for activation with N-methylmorpholine (NMM). NMM forms a morpholinium salt that acts as a good leaving group for the incoming carboxylic acid nucleophile that

displaces the NMM and transitions into its activated ester form while stationary on the resin. The final coupling step can be carried out using primary and secondary amines, creating an amide linkage and eluting through the bottom of the syringe (Figure 17).

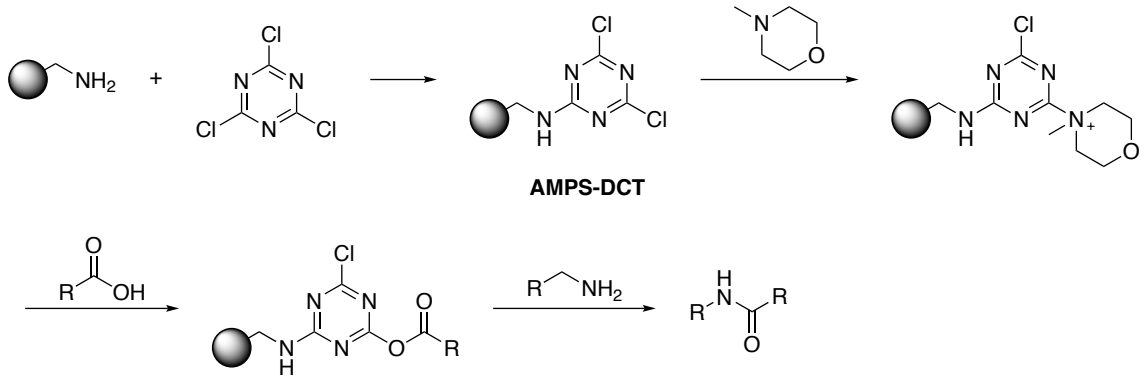

Figure 17. AMPS-DCT resin interaction scheme.

Following the procedure in Figure 18, compounds **16**, **13**, and **17** were immobilized on the AMPS-DCT resin in their respective activated ester forms, confirmed via the presence of visible fluorescence throughout the resin which indicated binding. Flow-through of the BODIPY dyes was controlled using the syringe apparatus to augment interactions between the carboxylic acid moiety and morpholinium salt in the cartridge. In about 2 mL of solvent, the flow-through time was extended for up to one hour to facilitate displacement of the morpholinium salt, and what was left on the resin was the AMPS-DCT-BODIPY

complex that can be used after a thorough rinse or stored for later use. Figure 18 illustrates the general coupling procedure used to generate **16a**.

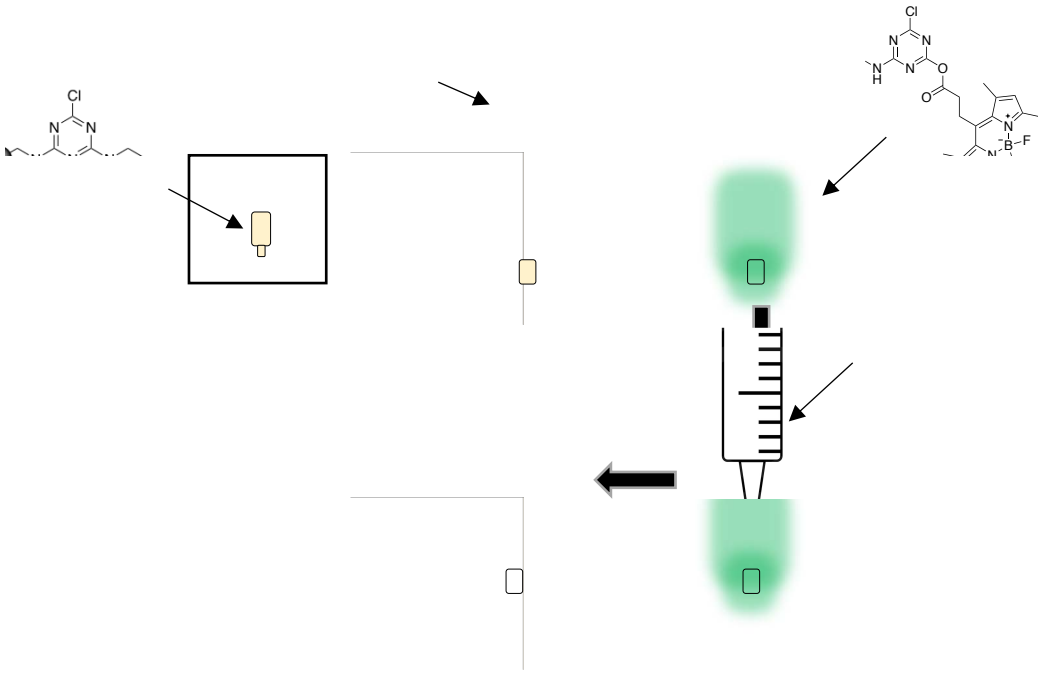

ure 18. Amide coupling of BODIPY fluorophores via AMS-DCT resin.

In order to test the scope with which the amide coupling reaction would be successful, a variety of amines were attempted with each BODIPY fluorophore in the AMPS-DCT resin. Morpholine (**a**), piperazine (**b**), hexylamine (**c**), pyrrole (**d**), and imidazole (**e**) were tested via amine flow-through of the AMPS-DCT-BODIPY resin complex in order to assess its availability for amide coupling. It was found that BODIPY compounds **16**, **13**, and **17** were successful in coupling to amines **a**, **b**, and **c**, resulting in the synthesis of nine BODIPY

derivatives with newly constructed amide linkage (Figure 19). Amines **d** and **e** were unsuccessful after numerous coupling attempts, most likely due to difficulties with access to resonance stabilized aromatic amines to participate in coupling. Additionally, N-acyl-imidazoles are reactive intermediates which are expected to have poor yields as they are prone to decomposition and hydrolysis.

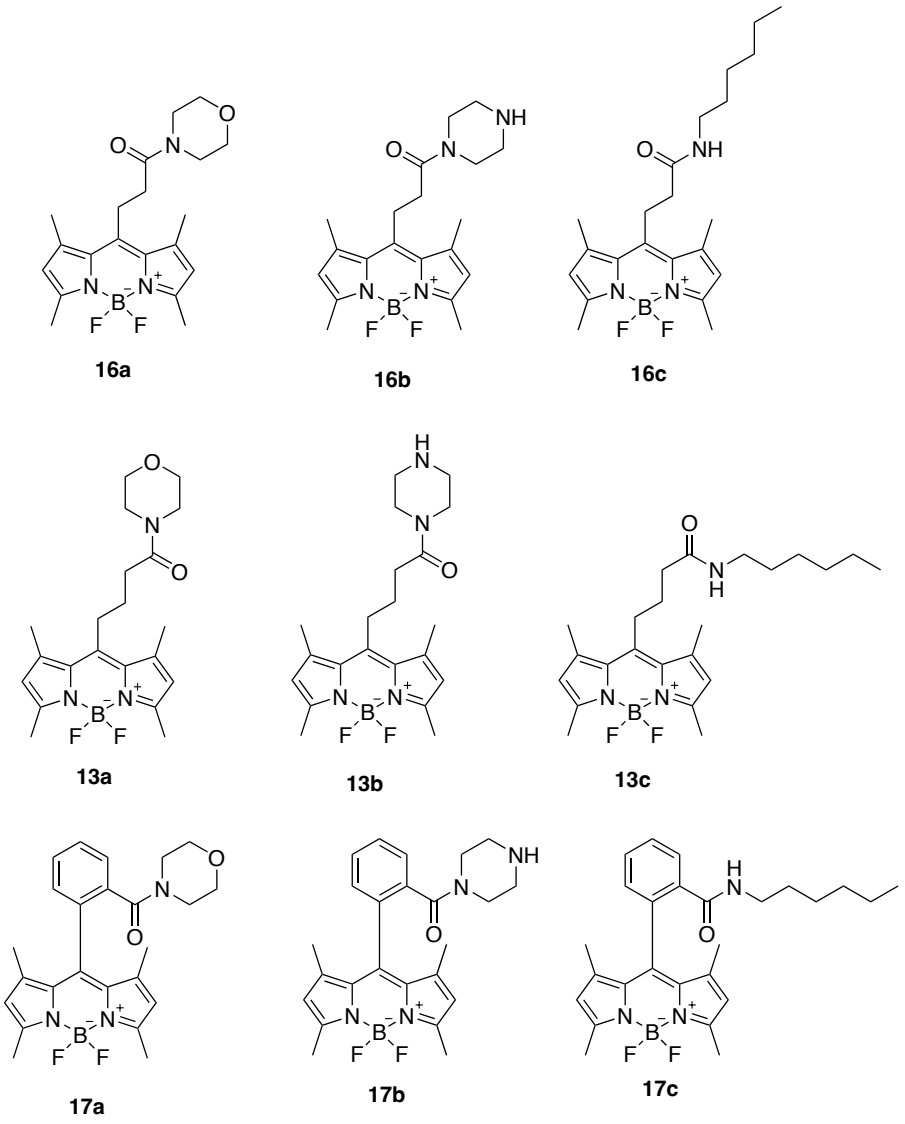

Figure 19. BODIPY derivatives/AMPS-DCT coupling products.

Due to the effectiveness of the BODIPY dye's fluorescent characteristics, relatively small amounts were used to test coupling ability with each amine. It was found that compound **17** was able to couple the most efficiently after immobilization on the AMPS-DCT resin, with percent yields up to 20% for **17b** (Table 1, Figure 19). On average, compound **13** appeared to have the most difficulty coupling to amines following immobilization, with yields as low as 2%. This may be attributed to suboptimal reaction conditions which did not provide proper orientation for incoming amine nucleophile. Each amine was attempted with the AMPS-DCT-BODIPY coupling technique a minimum of n=3 for a total of 60 coupling attempts and subsequently tested for UV excitation and emission spectra. Percent yield was calculated assuming 100% immobilization of BODIPY fluorophore on AMPS-DCT resin after saturation with dye. Based on the assumption that all of the BODIPY dye was retained on the resin for coupling, the per cent yield could be calculated after elution, purification, and mass determination of the final product. This is an assumption that reduces the percent yield to its lower limit. UV data was collected in CH_2Cl_2 solvation environment.

No significant change to percent yields was seen amongst coupling products for **13** which ranged from 5% to 6% (Table 1). A wider range was evident in coupling products of **16** as the average yield for **16a** was 7% which dropped to 4% for **16c**. As mentioned before, **17** saw the highest percent yields with averages as high as 12% for **17c**.

Table 1. Percent yield and UV spectra results for AMPS-DCT BODIPY amide coupling products.

Compound	Per cent Yield (avg, %)	λ_{max} (abs, nm)	λ_{max} (em, nm)	$\Delta\lambda$ (CH_2Cl_2, nm)
16	-	503	514	11
16a	7	501	511	10
16b	5	501	512	11
16c	4	503	511	8
13	-	502	510	8
13a	6	501	511	10
13b	5	500	510	10
13c	5	500	511	11
17	-	503	520	17
17a	9	507	518	11
17b	11	505	521	16
17c	12	506	517	11

2.3. AMPS-DCT Amide Coupling Effects on Photochemical Properties of Carboxy-BODIPY Dyes

Fluorescence data collected from each coupling product was plotted as normalized UV spectra to analyze any UV shifts of each derivative to the original BODIPY dye used for coupling. Due to BODIPY's insensitivity to solvent polarity

only CH_2Cl_2 was utilized as a medium for comparison.[29] Figure 20A shows little change in $\lambda_{max,abs}$ for coupling products of **13** (Table 1). The small changes in $\lambda_{max,em}$ seen in Figure 20B illustrate the variation in the emission profile for each compound which also resulted in slightly higher Stoke's shift ($\Delta\lambda_{max}$) values.

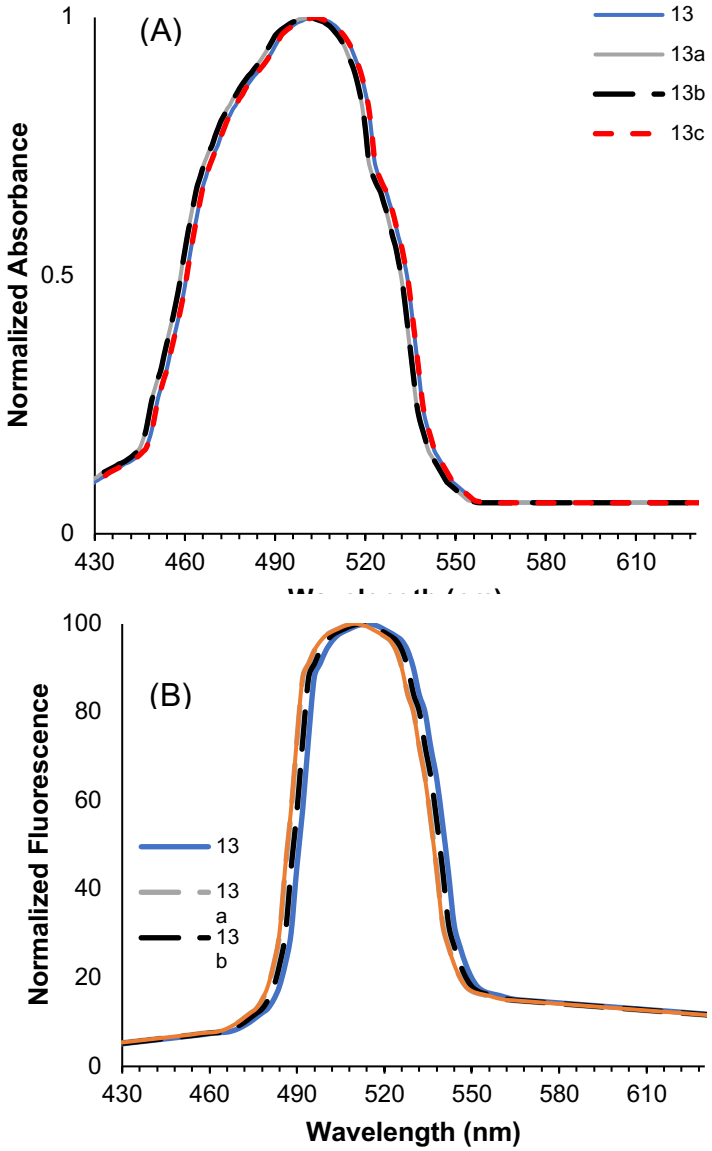

Figure 20. UV spectra for compound 13 coupling products.
(A) Normalized excitation spectra (ca. 1 x 10^{-5} M) in CH_2Cl_2; (B) Normalized fluorescence spectra (ca. 1 x 10^{-5} M) in CH_2Cl_2.

Normalized UV spectra for the excitation data of **16** (Figure 21A) and its derivatives shows a reduction in the $\lambda_{max,abs}$ for **16a** and **16b** (501 nm), and no changes for **16c** (503 nm). Compound **16c** showed a reduction in its $\Delta\lambda_{max}$ due to its $\lambda_{max,em}$ being shifted to 511 nm (Table 1). Compound **16b** was consistent with a blue shift compared to **16** and maintained a consistent $\Delta\lambda_{max}$ of 11 nm.

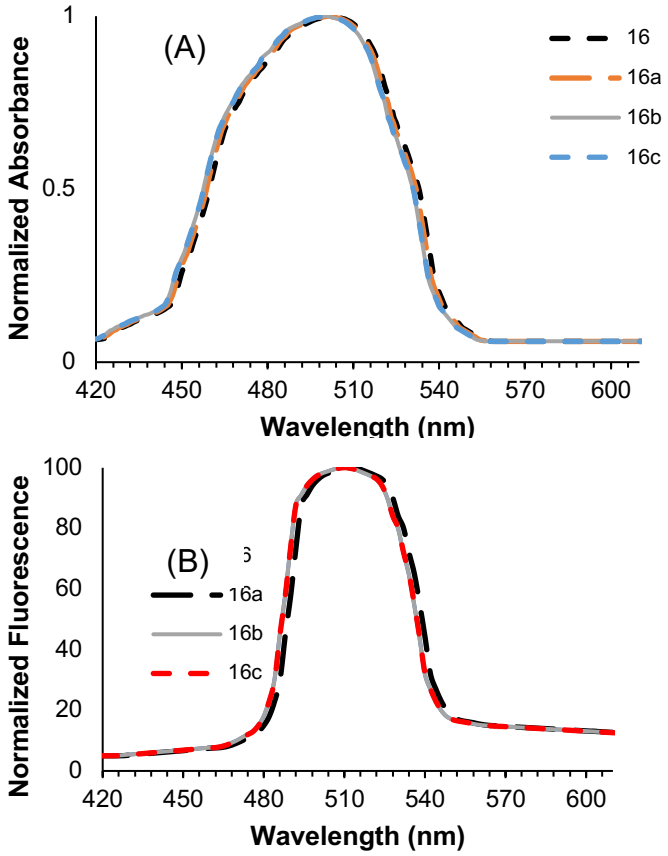

Figure 21. UV spectra for compound 16 coupling products. (A) Normalized excitation spectra (ca. 1 x 10^{-5} M) in CH_2Cl_2; (B) Normalized fluorescence spectra (ca. 1 x 10^{-5} M) in CH_2Cl_2.

The largest $\Delta\lambda_{max}$ is seen in compound **17** as well as its derivative **17b** (17 nm, 16 nm, respectively; Table 1). The coupling of amine **a** caused the $\Delta\lambda_{max}$ to decrease to 11nm, a similar hypsochromic shift to coupling with amine **c** which caused a blue-shifted excitation and emission profile (Figure 22). Although the $\Delta\lambda_{max}$ is larger than **13** and **16**, it is still significantly smaller than most other fluorophores.

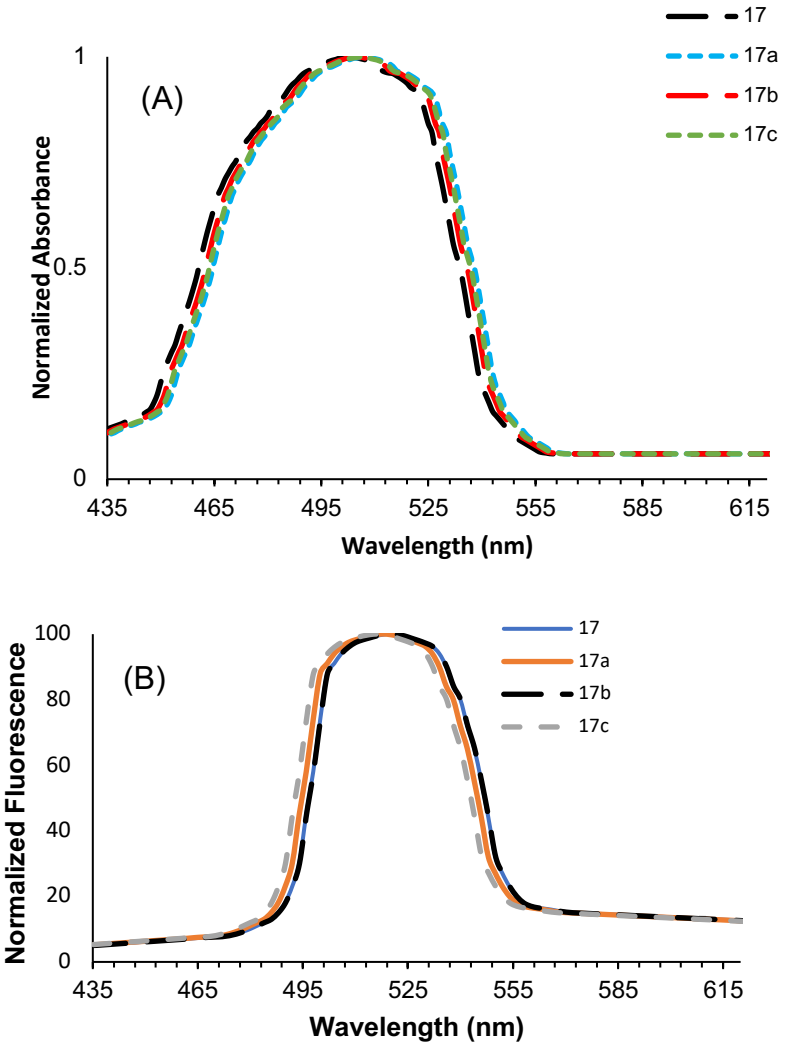

Figure 22. UV spectra of compound 17 coupling products. (A) Normalized excitation spectra (ca. 1 x 10^{-5} M) in CH_2Cl_2; (B) Normalized fluorescence spectra (ca. 1 x 10^{-5} M) in CH_2Cl_2.

3. DISCUSSION

3.1. Methodology

3.1.1. AMPS-DCT Amide Coupling Procedure

Commercially available SiliaBond Dichlorotriazine resin (Si-DCT) has been discontinued, and so a different solid support was achieved through the use of the commercially available AMPS resin. A small amount can be added to a 1 mL resin cartridge tube that is attached to a syringe which is then saturated with CH_2Cl_2 or CH_3CN as the solvent; the mole equivalency for the resin can be calculated based on the specific AMPS resin being used (in this case, 2.9 mmol/g). From this step, 5 mol equivalents of cyanuric chloride is dissolved in 20 mL of solvent and then flowed through via the syringe to ensure saturation of the AMPS resin. The resulting solid support is now an AMPS-DCT resin ready for activation with *N*-methylmorpholine (NMM).

The AMPS-DCT resin is then activated with 3 mol equivalents of NMM in 2mL of solvent to form the morpholinium salt. Finally, 2 mol equivalents of carboxylic acid were flowed through the resin cartridge in about 2 mL of solvent over 5 – 30 minutes to displace the morpholinium salt, immobilizing the carboxylic acid in its activated ester form to react with an amine and form the desired amide or be stored for use at a later date. Preparation of the AMPS-DCT resin was done in as little as 5 minutes but could be extended by manipulating the syringe to adjust elution rate.

The BODIPY compounds used showed relatively good solubility in normal concentrations with CH_2Cl_2, but such small volumes resulted in high concentrations of the carboxylic acid dye, causing increased viscosity of the solution which prevented proper flow through of the resin. Sonication was used in an attempt to dissolve all of the dye in the small volume (~2 mL) of solvent. Therefore, lower concentrations were used during the BODIPY loading phase which allowed for better flow through the resin. A consequence of this adjusted method could be that the BODIPY carboxylic acid doesn't saturate the resin completely, leaving some exposed morpholinium salt that would interact with the amine in the final step. To resolve this, approximately 5 mL of a 20% isopropanol/CH_2Cl_2 solution was flowed through the resin after the BODIPY loading phase in order to displace the morpholinium salt that was left on the resin with a sterically hindered group (Figure 23). Ideally, this isopropanol solution would not be able to displace the BODIPY in its activated ester form – this was confirmed via TLC of the products after rinsing the resin. Rates of flow could be controlled to induce longer resin interactions with reagents by using a syringe plunger. This created an airtight seal in the syringe allowing for complete control of flow-through.

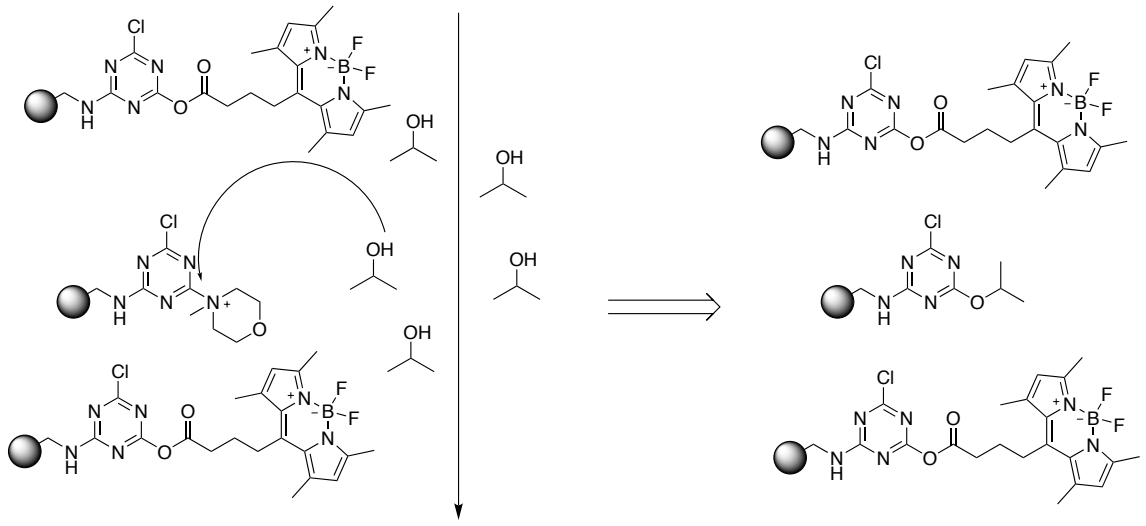

Figure 23. Isopropyl alcohol selectively displacing unreacted N-methyl morpholine with a sterically hindered isopropyl linkage.

The final step involved rinsing the resin to get rid of any unreacted carboxylic acid, dissolving about 2 equivalents of the chosen amine in CH_2Cl_2, and flowing the amine through the resin at a controlled rate via syringe plunger to enhance coupling interactions. The elution would contain the coupling product as well as some unreacted amine which could be discarded by employing a simple acid workup. The final product was dried and weighed after purification to allow for percent yield calculation; BODIPY loading onto resin was assumed to be 100% effective and treated as limiting reagent. This methodology was applied to each BODIPY dye and amine and represents a “worst case scenario” – the assumption that the loading of the BODIPY dye onto the resin is 100% successful is very unlikely. In reality, the yields calculated for each trial can be assumed to be the minimum yield possible.

3.1.2. Amino Acid Coupling Procedure

The AMPS-DCT general coupling procedure was adapted for two amino acids:

- **L-isoleucine** [$C_2H_5CH(CH_3)CH(NH_2)CO_2H$], and
- **H-Lys-(Boc)-OH** [$(CH_3)_3COCONH(CH_2)_4CH(NH_2)COOH$)]

The final coupling step with the amine suspended in solvent was replaced by an amino acid suspended in aqueous solution accompanied by the phase-transfer agent tetraethylammonium bicarbonate [$(CH_3CH_2)_4N(HCO_3)$]. In initial attempts, the solvent was changed to CH_3CN for its miscibility with the amino acid aqueous solution. Initial observations showed a decrease in resin swelling when using CH_3CN instead of CH_2Cl_2, affecting flow rate and consequently resin interactions. The reduced swelling of the resin consequently resulted in difficulties with the following steps as resin interactions were reduced due to increased flow rate through non-swollen resin The BODIPY dye was not able to be immobilized on the resin which was evident by the reduced fluorescence in the polypropylene filter tube.

Next trials found success loading the resin using CH_2Cl_2 as the solvent which allowed for maximum swelling and proper preparation of the AMPS-DCT-BODIPY complex. An isopropanol rinsing was conducted as normal, after which the resin was rinsed of CH_2Cl_2 using CH_3CN prior to the addition of the aqueous amino acid solution. No fluorescence was seen in the elution product for these attempts, and upon investigating the TLC and mass spectrometry results it can

be concluded that this procedure failed to couple the amino acid to a BODIPY fluorophore.

3.2. SPS Method Analysis

The primary goal of this study was to investigate an efficient SPS method which was able to attach BODIPY fluorophores to amine-functionalized compounds. This was achieved by evaluating the yields obtained from different BODIPY derivatives and amines to understand the impact of substituents on the efficiency of the coupling reactions. An SPS method was selected due to its advantages over traditional solution methods such as the simplicity of purification and potential for automation. It is particularly advantageous for synthesizing fluorescent probes because it allows for the systematic and controlled incorporation of fluorophores into a variety of molecules. Three carboxylic acid-functionalized BODIPY fluorophores were tested with this method and coupled to five amines, of which three were successful in forming amide linkage and maintaining fluorescence. This allowed for investigations into the impact BODIPY substituents have on coupling yields as well as the effect each type of amine had on yields. Photochemical data was also recorded for all coupling products which is useful in exploring the effect that BODIPY substituents have on the core.

Each BODIPY fluorophore was able to be synthesized by a two-step, one-pot reaction from acid anhydrides – compound **16** was afforded in 22% by 1,4-dimethyl pyrrole and succinic anhydride (Figure 13).[29] This yielded a methyl-

substituted BODIPY core with a propanoic substituent in the *meso* position, a slightly shorter chain than the butanoic substituent on compound **13**. A shorter aliphatic chain would have higher steric hindrance compared to a longer chain, effectively reducing the approachability of nucleophiles.[53] The shorter chain would also provide less flexibility during the reaction and may have more difficulties accommodating the spatial requirement of the coupling reaction, thereby decreasing the yield compared to a longer aliphatic chain.

The average yield of **16a** was 7%, slightly higher than **16b** (5%) and **16c** (4%, Figure 23, Table 1). The higher yield of **16a** may be due to steric accessibility of morpholine compared to piperazine and hexylamine; morpholine's structure provides less steric hindrance, allowing better access to reactive sites. The nitrogen in morpholine is also moderately basic and nucleophilic, which is efficient for coupling without excessive side reactions and sufficient to react readily with the activated carboxylic acid substituent. The presence of two nitrogen atoms on piperazine can lead to competing hydrogen bonding interactions and reduce overall efficiency of the coupling reaction.

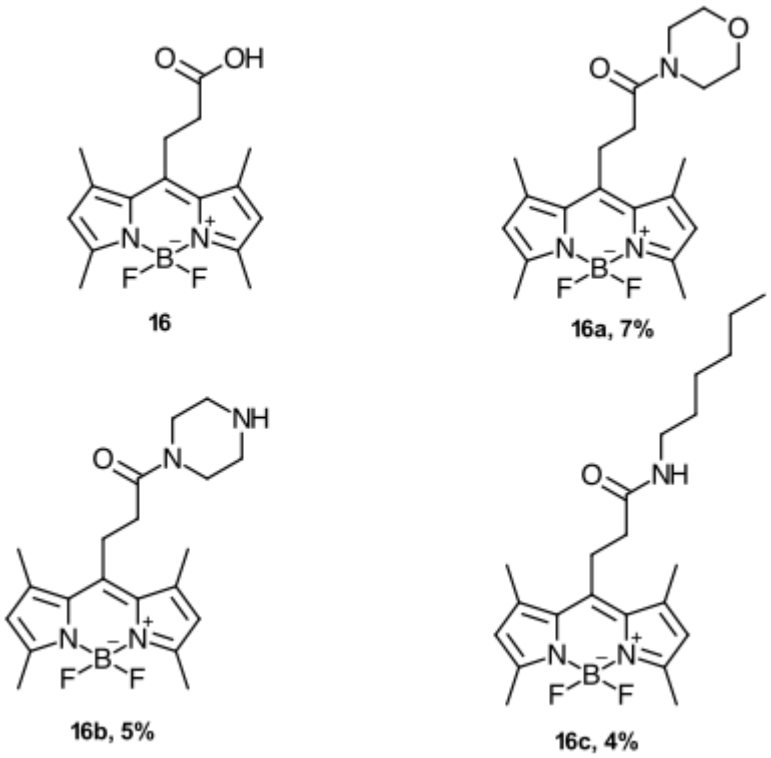

Figure 23. Structures and yields for compound **16** and its derivatives.

Compound **13** has a slightly longer chain than **16** located at the *meso* position of the BODIPY core due to its synthesis involving 1,4-dimethyl pyrrole and glutaric anhydride (20%, Figure 13). This synthesis afforded a butanoic acid substituent, allowing for more flexibility and less steric hindrance than the shorter propanoic acid substituent. As a result, the yields should follow the same trend as **16** but be slightly higher on average. It was observed that the coupling reaction with morpholine produced **13a** with a 6% yield, which was unexpectedly lower than the yield seen for **16a** (Table 1) but higher than the yields observed for **13b** (5%) and **13c** (5%, Figure 24, Table 1). A possible reason for **13a** having a lower yield than **16a** may be due to consequences of the longer chain and its

orientation; conformational variability of **13** caused by the flexible aliphatic chain while it is immobilized on the resin may not always have the carboxylic group in the optimal orientation for nucleophilic attack. When comparing the yields of compound **13** derivatives, they followed the same trend seen for **16** but showed a decrease in deviation between average yields, implying that the differences between cyclic and acyclic amines do not have as much of an effect on coupling rates for **13** as **16**.

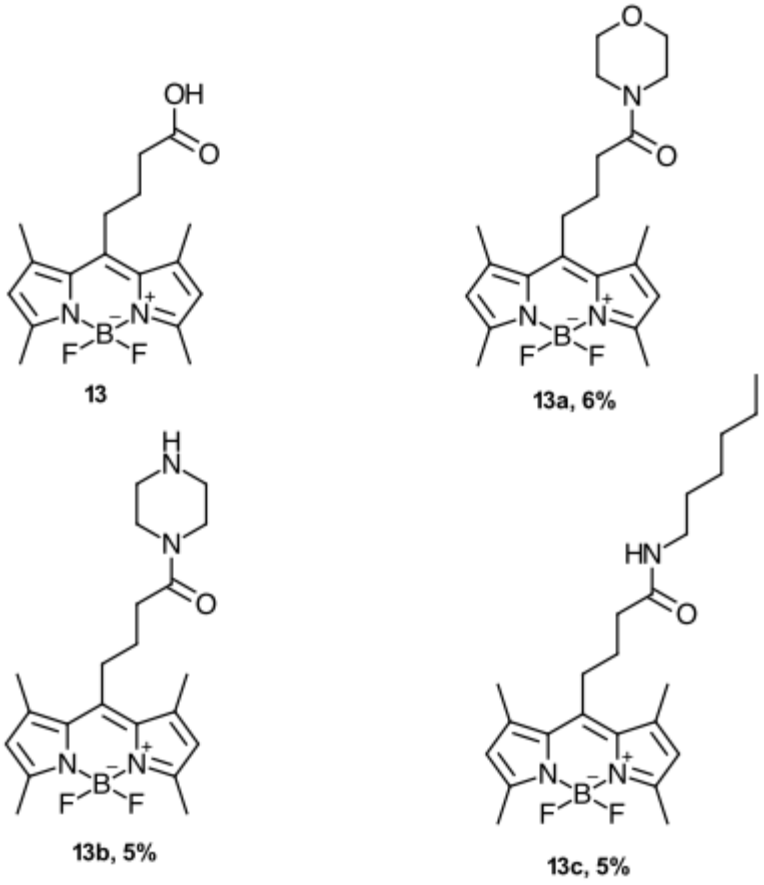

Figure 24. Structures and yields for compound **13** and its derivatives.

It should be noted that the smaller size and flexibility of morpholine contribute to its higher efficiency in coupling reactions when compared to piperazine and hexylamine.[54] Although compound **13** gave lower yields than **16** despite its longer chain, morpholine was still able to couple and produce a higher yield than piperazine and hexylamine for both **13** and **16**. All three amines showed good solubility in CH_2Cl_2 and reaction times were consistent across all trials allowing for maximum resin interactions. Additionally, all purification steps were consistent with a quick acid wash to get rid of unreacted amine and drying the final product to ensure there is no contamination.

The final BODIPY fluorophore that was synthesized to test the SPS method was functionalized with a 2-benzoic acid substituent in the *meso* position. Compound **17** was constructed using the same scheme but substituting the glutaric and succinic anhydride for phthalic anhydride which yielded 27% of a bright orange dye as the final product (Figure 13). It was expected that, because of the aromatic substituent, compound **17** would not couple efficiently on a resin using the SPS method and would have the lowest yields. On the contrary, it was found that **17** coupled to morpholine (**17a**, 9%), piperazine (**17b**, 11%), and hexylamine (**17c**, 12%) significantly more efficiently than dyes **16** or **13** (Figure 25, Table 1).

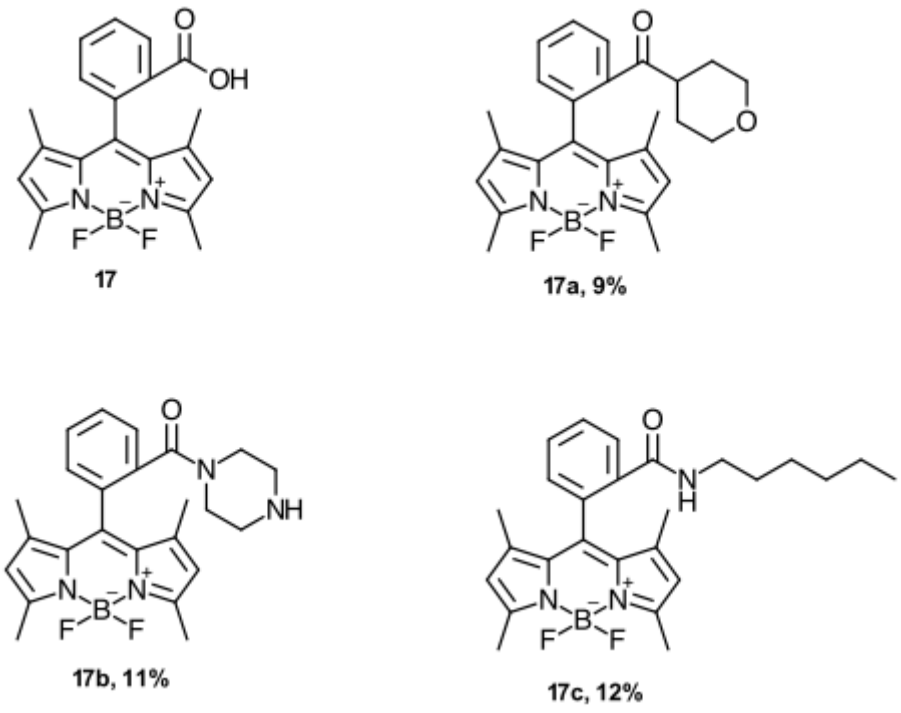

Figure 25. Structures and yields of compound **17** and its derivatives.

A reasonable explanation for the results seen for compound **17** draws upon the planar structure and aromaticity of the benzoic acid substituent; this would allow it to engage in $\pi - \pi$ stacking interactions which can facilitate the approach and proper orientation of the amine nucleophile during the coupling reaction. This would also allow for stabilization of reaction intermediates through extended conjugation in the aromatic group, that most likely promoted efficient coupling.[55] Additionally, the electron-withdrawing nature of the aromatic ring most likely increased the electrophilicity of the carbonyl carbon in the ester group as the fluorophore was immobilized on the resin, making the ester more susceptible to nucleophilic attack by the amine.

It is possible that, despite its success in coupling to **16** and **13**, morpholine ran into steric hindrance in the S_N2 reaction during attempts with **17**. As morpholine and piperazine both have cyclic structures, their approach to the immobilized ester form of the benzoic acid substituent may have been more difficult than what was experienced by the long-chained, flexible structure of hexylamine. The nucleophilicity of hexylamine may also be a contributing factor in the yield for **17c**, however as mentioned before morpholine is also a successful nucleophile, therefore the most likely reason is attributed to steric considerations and the conformation of the BODIPY complex on the resin.

3.3. UV Spectra Analysis

The choice of amines for the coupling procedure was based on their varying structural and chemical properties. For example, morpholine and piperazine are both heterocyclic amines that tend to have an electron-donating effect on the BODIPY core, resulting in red shifts for both excitation and emission.[56] As a primary aliphatic amine, hexylamine coupling would introduce a flexible, long-chain substituent to the BODIPY core. The expected coupling results would be more minimal blue shifts when compared to conjugated and heterocyclic systems.[57] Therefore, results expected for BODIPY derivatives coupled to morpholine and piperazine (**13a, 13b, 16a, 16b, 17a, 17b**) should exhibit a red-shifted UV-spectrum compared to the parent compound; derivatives coupled to hexylamine (**13c, 16c, 17c**) should exhibit a blue-shifted UV-spectrum.

3.3.1. UV Analysis of Compound 13

As previously mentioned, the nitrogen-containing heterocyclic morpholine substituent can influence the photophysical properties of BODIPY fluorophores by increasing the electron density, leading to enhanced conjugation. The result of morpholine-substituted dyes include high fluorescence quantum yields and photostability.[58] When coupled with compound **13**, a slight increase in the Stokes shift was seen (10 nm) compared to its uncoupled parent compound (8 nm, Table 1). Upon further examination of the fluorescence data, **13a** showed a decrease from 502 nm for the uncoupled parent fluorophore to 501 nm, a small hypsochromic blue shift. The emission profile slightly increased from 510 nm to 511 nm, a small bathochromic red shift which was to be expected by a morpholine substituent (Figure 19, Table 1). Amide coupling of compound **13** with piperazine resulted in a slightly larger hypsochromic shift to 500 nm in **13b's** absorbance profile, however the emission profile remained unchanged at 510 nm (Figure 26, Table 1). Compound **13c** showed an absorbance and emission profile of 500 nm and 511 nm, respectively, after coupling with hexylamine. This illustrates a hypsochromic shift in the absorbance profile and a bathochromic shift in the emission profile as well as the largest Stokes shift seen for derivatives of compound **13**. As hexylamine is a primary aliphatic amine, it's long and flexible structure usually results in hypsochromic/blue shifts in absorbance and emission data compared to morpholine and piperazine.

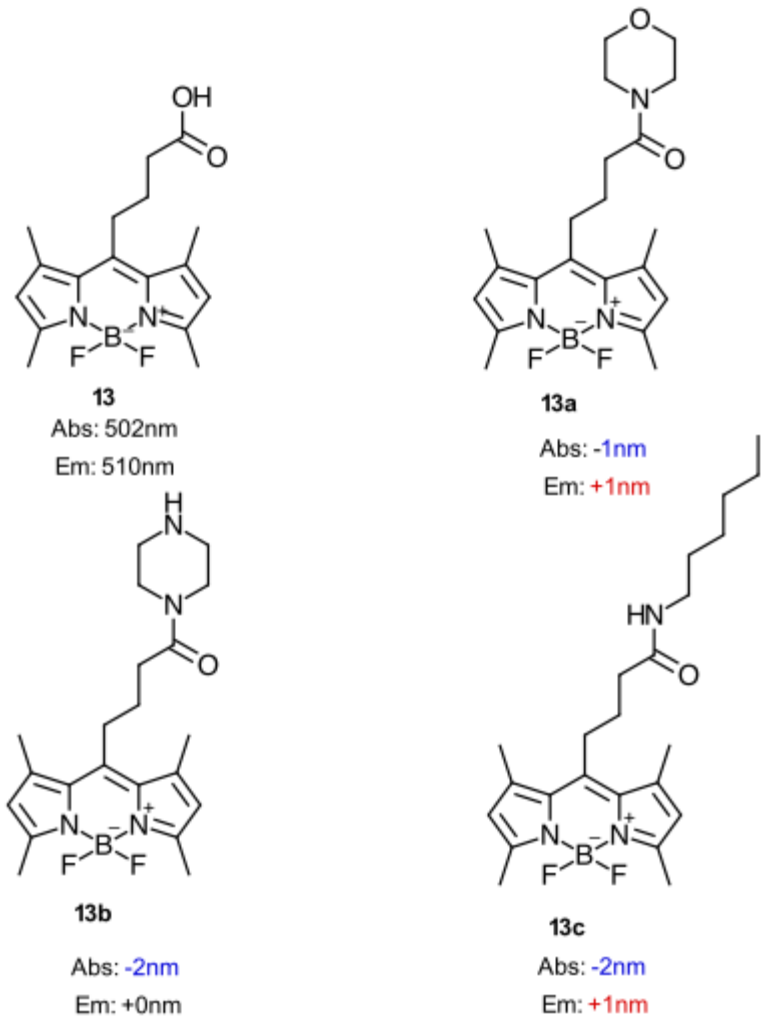

Figure 26. UV data for each derivative of compound 13.

3.3.2. UV Analysis of Compound 16

Compound **16a** showed a slight hypsochromic shift in its absorbance after coupling with morpholine, shifting from 503 nm to 501 nm (Figure 20, Table 1). A similar hypsochromic shift was seen in the emission profile of **16a**, decreasing its wavelength from 514 nm to 511 nm and decreasing the overall Stokes shift to 10 nm (Figure 27, Table 1). These findings are not consistent with the expected

results – the introduction of a morpholine substituent should have facilitated a bathochromic red shift in the excitation and emission data. One possible explanation for this anomaly is the potential alteration of energies between the HOMO and the LUMO – if morpholine was able to stabilize the HOMO more than the LUMO after coupling, the energy gap between the orbitals would increase, resulting in a hypsochromic blue shift in excitation and emission profiles of **16a**.[58] Coupling product **16b** showed a similar pattern with its piperazine substituent, exhibiting a hypsochromic shift in both excitation and emission (501 nm and 512 nm, respectively). Though this is also contrary to what the expected fluorescence profile should be, it may be explained by suboptimal electronic interactions and slight inductive effects between the BODIPY fluorophore and piperazine, similar to **16a**. The introduction of hexylamine for **16c** did not change the excitation profile of the fluorophore, indicating that the substituent did not have a significant impact on absorbance (503 nm). A hypsochromic shift in the emission profile is expected after the attachment of the long-chained amine and resulted in a reduction in the Stokes shift (511 nm, 8 nm).

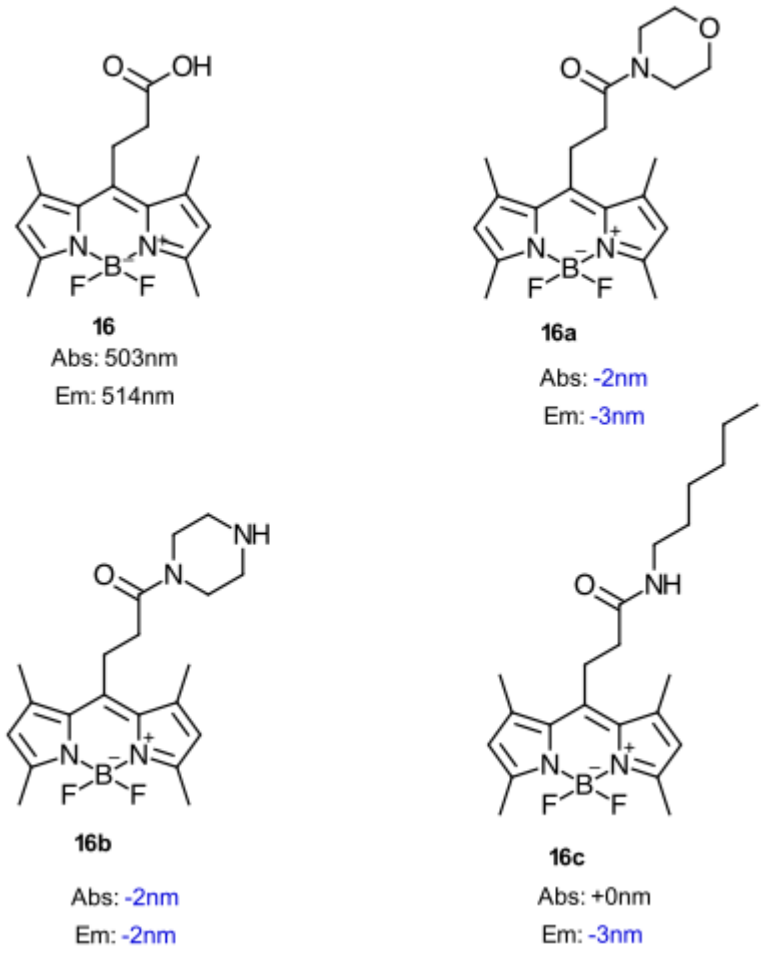

Figure 27. UV data for each derivative of compound 16.

3.3.3. UV Analysis of Compound 17

Analysis of the fluorescence profiles of compound **17** coupling products also contains results contrary to what was expected. The excitation profile of compound **17a** shows a bathochromic shift to 507 nm which is to be expected when undergoing coupling with a morpholine substituent (Figure 21, Table 1), however the emission profile showed a slight hypsochromic shift to 518 nm which reduced the Stokes shift from 17nm in compound **17** to 11 nm, a

significant decrease. The large Stokes shift seen in compound **17** was maintained when coupled to piperazine, giving an excitation and emission profile of 505 nm and 521 nm in compound **17b**, respectively. This is consistent with the expected bathochromic shift when coupled to piperazine and resulted in a similar Stokes shift in compound **17b** (16 nm, Figure 28, Table 1). Finally, a slight hypsochromic shift was seen in the excitation profile of **17c** which contained a hexylamine substituent, indicating that hexylamine had a red-shifted effect on the BODIPY core. Typically, the addition of a hexylamine substituent would cause a blue shift – this is seen in the emission profile of **17c**, which shifted from 520 nm to 517 nm. Although the red-shift in absorption is unexpected, the UV spectra analysis of **17c** show results that are consistent with the expected minimal electronic interaction and conjugation effects of the hexylamine substituent. No conjugation would be possible due to the “insulating” hydrocarbon chain separating the BODIPY core and the hexylamine substituent, which would also reduce inductive effects. This implies that a hexylamine substituent induces only minor changes to photophysical properties of BODIPY fluorophores.

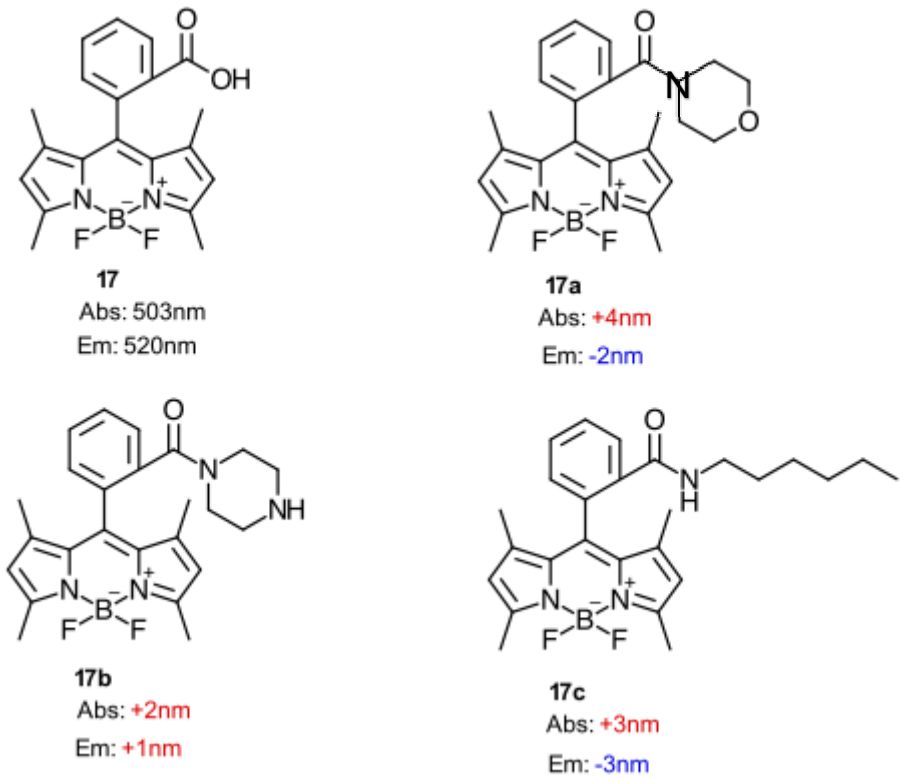

Figure 28. UV data for each derivative of compound **17**.

To summarize, the introduction of morpholine and piperazine caused slight blue shifts in emission profiles of the BODIPY coupling derivatives from **13** and **16**. This suggest very minimal inductive effects due to the small nature of the shifts seen. In turn, the expected red shifts were seen when morpholine and piperazine were coupled to compound **17**; these compounds saw the absorption of light at higher wavelengths, which indicates the presence of an aromatic substituent was favorable for increased conjugation and participated in the electron donating effects originating from the amines. Hexylamine substituted derivatives (**13c**, **16c**, **17c**) displayed minimal shifts in both excitation and emission spectra, which is characteristic of its flexible, non-conjugated nature.

They were able to maintain high fluorescence efficiency and stability with minimal perturbation of the versatile BODIPY core.

The thorough UV spectra analysis conducted on these BODIPY compounds provided valuable insights into how an array of amine substituents influenced the photophysical properties of the parent compounds. These findings emphasize the importance of considering electronic and steric factors when designing BODIPY-based fluorophores.

3.4. Experimental Limitations and Future Work

It is important when conducting research to view results through an objective lens – this allows for accountability and opens the door for improvements to methods and reproducibility. This study only looked at three different BODIPY fluorophores that varied in the carboxylic acid substituent of each. As a result, the limited range of BODIPY compounds may not provide a comprehensive evaluation of possible effects that the SPS coupling reaction could have on photophysical properties of all BODIPY compounds. Although the carboxylic acid substituents were necessary for participation in the coupling reaction, future research could expand on the substitution of the BODIPY core – a carboxylic acid substituent in the alpha or beta positions may affect the compounds coupling ability, as well as substituting the methyl groups around the BODIPY core with aryl, aromatic, or heteroaryl groups. Further substitution may improve interactions of BODIPY fluorophores in the resin and allow for increased immobilization, leading to higher yields.

As the selection of BODIPY fluorophore candidates for the SPS coupling reaction was strategically planned, the selection of amines was also by design. Morpholine, piperazine, hexylamine, pyrrole, and imidazole were selected to represent heterocyclic, aliphatic, and aromatic compounds and encompass a broad range of amines that may act as nucleophiles in the SPS coupling reaction. It was deduced that aromatic compounds had difficulty in coupling to the BODIPY fluorophores via this method, probably due to their ability to stabilize and avoid deprotonation under mild conditions which would decrease their nucleophilic character and not allow for efficient coupling to take place. The resistance of aromatic amines to the coupling reaction was not further explored and could be investigated in future research.

In mentioning the mild conditions of the reaction, it is important to note that the detailed SPS coupling method outlined in section 2.1. did see slight variations of reaction conditions during the coupling attempts. Some trials went slightly longer than others due to the packing and swelling of the resin, which allowed for longer interaction time and may have affected the yields. Also, all reactions were done at room temperature with room temperature solvents. Future work should focus on optimization of reaction conditions while following the general outline of the method, systematically varying the key parameters and documenting their effects to analyze efficiency and reproducibility. For example, increasing the environmental and solvent temperatures may increase the interactions necessary for the S_N2 reaction to occur, thereby increasing

yields. Additionally, varying the pH of the reaction and facilitating harsher conditions may allow for aromatic amines to participate in the coupling reaction.

It should be noted that the yields obtained in the coupling reaction trials are to be considered the lowest possible attainable – the loading of the BODIPY dyes onto the AMPS-DCT resin was considered to be 100% successful and in line with manufacturing maximums (2.9 mmol/mg). This is very unlikely, and it is expected to be much lower than 100%. Any future investigations should look into determining the actual amount of dye that is immobilized on the resin prior to amine coupling. One method would be utilizing UV visible spectroscopy to determine the absorbance of a BODIPY solution – of which the concentration is known – prior to flow through. The elution would then be collected, purified, and the BODIPY would be suspended in the exact same volume to measure its absorbance. The change in absorbance would be directly related to a change in concentration and the amount of BODIPY immobilized on the resin could be deduced. However, the yield results do provide a minimum baseline to work from and also reproducible efficiency when performing the reaction.

Section 2.3. illustrates the methods used to attempt the coupling reaction of the BODIPY fluorophores with two amino acids – these amino acids were selected based on availability and accessibility in the lab. Various attempts were made to successfully couple the amino acids to a BODIPY fluorophore; different solvents were used to account for solubility and resin interactions were optimized by controlled reaction periods. Although attempts were unsuccessful,

this work did show that coupling was successful for numerous types of amines, therefore future work should focus on optimizing the reaction conditions to successfully couple the BODIPY fluorophores to amino acids. This opens the door for biological applications and investigations into the practical applications of BODIPY-labeled compounds in biological systems. This could include cell imaging, *in vivo* tracking, and diagnostic assays that demonstrate the utility of the synthesized probes.

In summary, some of the flaws that were present in this study provide the groundwork for future research to improve on these methods. By addressing them and implementing the suggested improvements, future studies can build upon the foundation and contribute to the advancement of SPS methods in synthesizing fluorescent probes.

4. CONCLUSION

The primary goal of this study was to test the effectiveness of SPS in coupling amine-functionalized compounds to carboxylic acid functionalized BODIPY fluorophores. This method of developing fluorescent probes is a growing area of interest, so the development of an efficient SPS technique would have broad and impactful implications. It was found that the three BODIPY fluorophores tested using the AMPS-DCT resin technique were able to be immobilized on the resin and required an additional rinsing with isopropanol. The coupling reaction resulted in nine newly synthesized derivatives, three from each of the parent BODIPY compounds. Compound **17** participated in the coupling reaction with the highest yields which was potentially facilitated by its orientation on the resin and electronic stabilization by its aromatic benzoic acid substituent. On average, BODIPY compounds coupled to hexylamine showed the largest yields, most likely due to hexylamine's nucleophilic nature and flexibility. Photophysical analysis revealed that although some shifts were seen in the excitation and emission profiles, the relative Stokes shift seen in each parent compound was maintained in the derivatives after coupling to the amines. This demonstrates the resistance of the BODIPY core and how it can maintain its attractive photochemical properties despite undergoing rigorous coupling reactions with large substituents. This study contributes significantly to the field of fluorescent probe development – the short and efficient SPS method described here provides an alternative to classical solution-based chemistry and

opens the door to new, innovative routes to attaching fluorescent probes. The findings in this study should be considered when investigating future advancements in fluorescent probe development, as well as their diverse applications in science and medicine.

5. EXPERIMENTAL

5.1. General Methods

All reagents and solvents were obtained from a variety of suppliers and used without further purification, except for CH_2Cl_2 which was dried over 4A molecular sieves prior to each use. Organic layers collected from separatory funnels were dried using $MgSO_4$ and gravity filtered. Column chromatography was the main purification technique used and was conducted using SiliaFlash P60 40-63 μm (230-400 mesh) silica gel. UV-vis spectroscopy data was recorded using Perkin Elmer LS50B with FLDM Ver 3.00 software and 3 mL quartz cuvette for CH_2Cl_2 solutions. Samples were diluted to 1 x 10^{-5} M prior to testing and all excitation and emission data was normalized to the maximum peak for ease of comparison and wavelength shift analysis. NMR spectra were obtained with a 500 MHz Bruker Advanced Neo spectrometer and analyzed with Bruker TopSpin 4 software. 1H NMR was performed using 16 scans, while 13C NMR was performed using 1024 scans with power gated decoupling. 1H NMR chemical shifts are reported in parts per million (PPM) based on an internal standard of tetramethylsilane (TMS) set to δ 0.00 ppm. 13C NMR checmical shifts are reported in parts per million (ppm) based on the $CDCl_3$ solvent residual peak as an internal standard set to δ 77.16. Mass spectra were acquired with an Advion Expression CMS spectrometer in atmospheric chemical pressure ionization (APCI) mode and introduced using the atmospheric solid analysis probe (ASAP)

or an HPLC-MS system consisting of a WQaters 1525 Binary HPLC pump with an Xselect CSH C18 5 μm column attached to a Waters Acuity QDa mass detector.

The AMPS-DCT coupling procedure followed a general scheme which was slightly modified with an additional rinsing of 20% isopropanol/CH_2Cl_2 (see section 4.3). The procedure begins by adding a measured amount of aminomethyl polystyrene (AMPS, 100-150 mg) resin to a 5 mL filter tube and rinse with CH_2Cl_2 to allow the resin to swell in the tube. AMPS resin has a manufacturer's stated molar equivalency of 2.9 mmol eq/g – flow through 5 equiv cyanuric chloride in ~20 mL CH_2Cl_2 to convert AMPS resin to AMPS-DCT. The next step is flowing through 3 equiv NMM in ~2 mL CH_2Cl_2 and then 2 equiv of the carboxylic acid in ~2 mL CH_2Cl_2. It is recommended to rinse the resin after each flow-through with a small amount of solvent to get rid of any unreacted compound. At this point, prepare the target amine at 1.5 – 2 equiv in ~2mL CH_2Cl_2, flow through resin filter tube and collect elution in clean beaker. A quick acid workup of the elution will afford the final product that can be extracted with CH_2Cl_2 and then dissolved.

5.2. Chemical Procedures

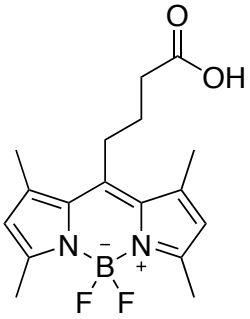

4-(4,4-Difluoro-1,3,5,7-tetramethyl-4-bora-3a,4a-diaza-s-indacene-8-yl)-butyric Acid (13). In a round bottom flask, a mixture of glutaric anhydride (200 mg, 1.75 mmol), dry CH_2Cl_2 (30 mL), 2,4-dimethylpyrrole (280 mg, 3 mmol), and BF_3OEt_2 (0.51 g, 3.6 mmol) was added sequentially. The mixture was heated to reflux for 18 h under N_2, then allowed to cool to room temperature. Once cooled, Et_3N (1.21 g, 12 mmol) and BF_3OEt_2 (1.28 g, 9 mmol) were added slowly, and the mixture stirred under reflux/for another 12 h. The resulting solution was washed with water (3 x 15 mL) prior to drying over $MgSO_4$. The solvent was removed via rotary evaporation which afforded a dark red oil that was purified by column chromatography silica gel (hexane/EtOAc, 2:1) to yield 120 mg of a maroon-red solid (24% yield). Fluorometer investigations into excitation and emission found 502 nm/510 nm ($\lambda_{max,abs}/\lambda_{max,em}$). MS (APCI) *m/z* calculated for $C_{17}H_{21}BF_2N_2O_2$ 334.1 found 333.2 M (- COOH proton). ^{1}H NMR ($CDCl_3$, 500 MHz) δ 10.22 (s, 1H, -COOH), 6.12 (s, 2H, pyrrole-H), 3.00 (t, 2H, -CH_2, *J* = 6.4 Hz), 2.67 (t, 2H, -CH_2, *J* = 6.4 Hz), 2.52 (s, 6H, -CH_3), 2.29 (s, 6H, -CH_3), 2.20-2.12 (m, 2H, -CH_2); ^{13}C NMR ($CDCl_3$, 125 MHz) δ 178.2, 153.5, 150.6, 146.6, 133.8, 118.1, 34.1, 22.3, 21.1, 18.8, 14.3.

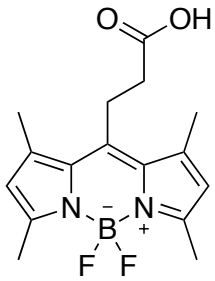

3-(4,4-Difluoro-1,3,5,7-tetramethyl-4-bora-3a,4a-diaza-s-indacene-8-yl)-propanoic Acid (16). To a round-bottom flask was added succinic anhydride (200 mg, 2.0 mmol), dry CH_2Cl_2 (20 mL), dry CH_3CN (5 mL), and 2,4-dimethylpyrrole (457 mg, 4.80 mmol). The mixture was refluxed under N_2 for 18 h and was allowed to come down to room temperature before slowly adding 6 equiv of Et_3N (1.21 g, 12 mmol) and 8 equiv of BF_3OEt_2 (2.27 g, 16 mmol), respectively. The reaction was stirred under N_2 at 50°C for another 12 h then quenched and washed with water (3 x 15 mL). The organic phase was dried over anhydrous $MgSO_4$, and the solvent was evaporated via vacuum rotary evaporator leaving a dark reddish-brown crude product. Column chromatography purification on silica gel (CH_2Cl_2/EtOAc, 2:1) yielded 140 mg of a dark red solid (22% yield). Fluorometer investigations into excitation and emission found 503 nm/514 nm ($\lambda_{max,abs}/\lambda_{max,em}$). MS (APCI) *m/z* calculated for $C_{16}H_{19}BF_2N_2O_2$ 319.1 found 318.1 (M - COOH proton). ^{1}H NMR ($CDCl_3$ 500 MHz) δ 6.01 (s, 2H, pyrrole-H), 3.40 (t, 2H, -CH_2, *J* = 6.4 Hz), 2.32 (t, 2H, -CH_2, *J* = 6.4 Hz), 2.51 (s, 6H, -CH_3), 2.20 (s, 6H, -CH_3). ^{13}C NMR ($CDCl_3$, 125 MHz) δ 178.9, 152.0, 149.8, 145.8, 134.2, 122.1, 32.7, 22.2, 16.6, 14.4.

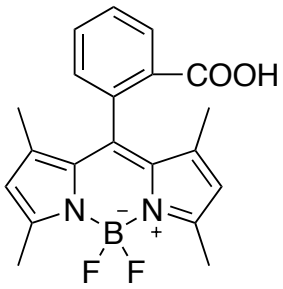

2-(4,4-Difluoro-1,3,5,7-tetramethyl-4-bora-3a,4a-diaza-*s*-indacene-8-yl)-benzoic Acid (17). *o*-Phthalic anhydride (296 mg, 2 mmol) and 2,4-dimethylpyrrole (380 mg, 4 mmol) were added to a nitrogen flushed 100 mL RBF and dissolved in CH_3CN (20 mL). The solution was attached to a reflux condenser and heated to 60 °C for 12 h under N_2. The solution was then allowed to cool to room temperature, and 6 equiv Et_3N (1.21 g, 12 mmol), followed by 8 equiv of BF_3OEt_2 (2.27 g, 16 mmol), was added dropwise into the reaction mixture, respectively. The solution was allowed to stir under nitrogen at 50 °C for 4 h, and another 14 h at room temperature. Finally, the reaction mixture was washed with water (3 x 15 mL), extracted with CH_2Cl_2, dried over $MgSO_4$, and the solvent was evaporated via rotary evaporation to afford a dark red-orange oil. This crude product was purified via column chromatography silica gel (hexane/EtOAc/MeOH 100:30:3) and yielded 189.5 mg of dark orange powder (26% yield). Fluorometer investigations into excitation and emission found 503 nm/520 nm ($\lambda_{max,abs}/\lambda_{max,em}$). MS (APCI) *m/z* calculated for $C_{20}H_{19}BF_2O_2N_2$ 368.1 found 367.2 (M - COOH proton). ^{1}H NMR ($CDCl_3$, 500 MHz) δ 12.93 (s, 1H, COOH), 7.87 (dd, *J* = 7.5 Hz, 1H), 7.81 (dd *J* = 7.0 Hz, *J* = 2.1 Hz, 1H), 7.46 (dd, *J* = 7.0 Hz, *J* = 2.1 Hz, 1H), 7.29 (dd, *J* = 7.0 Hz, 1H), 6.28 (s, 2H, pyrrole-2H), 2.54 (s, 6H, -CH_3), 2.24 (s, 6H, -CH_3); ^{13}C NMR ($CDCl_3$, 125 MHz) δ 168.2, 153.0, 142.9, 142.2**,** 136.0, 134.3, 129.5, 129.2, 129.0, 128.7, 128.2, 121.0, 13.9, 13.5.

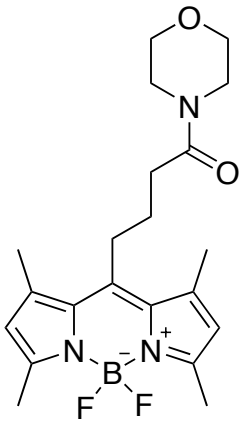

4-(4,4-Difluoro-1,3,5,7-tetramethyl-4-bora-3a,4a-diaza-s-indacene-8-yl)-1-(morpholin-4-yl)butan-1-one (13a). The synthesis followed the AMPS-DCT amide coupling procedure (section 5.1) using **13** as the carboxylic acid and morpholine **a** as the amine. Fluorometer investigations into excitation and emission found 501nm/511nm ($\lambda_{max,abs}/\lambda_{max,em}$). MS (APCI) *m/z* calculated for $C_{21}H_{28}BF_2N_3O_2$ 403.2 found 403.1 (M). ^{1}H NMR ($CDCl_3$, 500 MHz) δ 6.43 (s, 2H, pyrrole-H), 3.67 (t, 4H, -CH_2, *J* = 4.2 Hz), 3.38 (m, 4H, -CH_2), 2.94 (t, 2H, -CH_2, *J* = 6.1 Hz), 2.50 (s, 6H, -CH_3), 2.44 (t, 2H, -CH_2, *J* = 6.1 Hz) 2.27 (s, 6H, -CH_3) 1.93 (t, 2H, -CH_2, *J* = 6.1 Hz); ^{13}C NMR ($CDCl_3$, 125 MHz) δ 169.6, 154.4, 146.6, 133.9, 128.1, 122.3, 66.5, 44.4, 35.5, 28.5, 23.0, 18.8, 14.2.

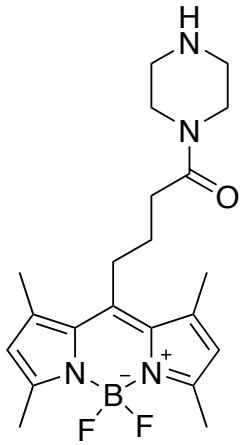

4-(4,4-Difluoro-1,3,5,7-tetramethyl-4-bora-3a,4a-diaza-s-indacene-8-yl)-1-(piperazin-1-yl)butan-1-one (13b). The synthesis followed the AMPS-DCT amide coupling procedure (section 5.1) using **13** as the carboxylic acid and piperazine **b** as the amine. Fluorometer investigations into excitation and emission found 500nm/510nm ($\lambda_{max,abs}/\lambda_{max,em}$). MS (APCI) *m/z* calculated for $C_{21}H_{29}BF_2N_4O$ 402.2 found 402.0 (M). ^{1}H NMR ($CDCl_3$, 500 MHz) δ 6.40 (s, 2H, pyrrole-H), 3.87 (t, 2H, -CH_2, *J* = 9.5 Hz), 3.48 – 3.41 (m, 4H, -CH_2), 3.08 (m, 4H, -CH_2), 2.90 (d, 2H, -CH_2, *J* = 7.4 Hz), 2.78 (s, 6H, -CH_3), 2.44 (s, 6H, -CH_3), 2.02 (t, 2H, -CH_2, *J* = 7.4 Hz), 1.92 (s, 1H, -NH); ^{13}C NMR ($CDCl_3$, 125 MHz) δ 172.2, 156.3, 144.5, 139.8, 129.4, 122.1, 46.0, 44.9, 29.2, 27.4, 15.9, 14.2, 12.6.

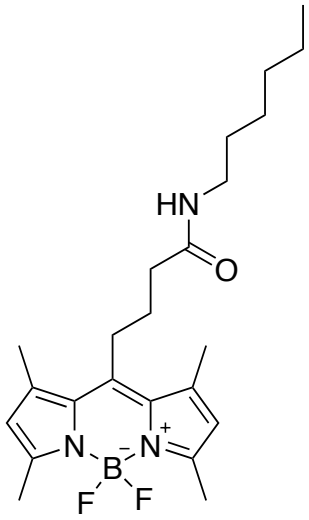

4-(4,4-Difluoro-1,3,5,7-tetramethyl-4-bora-3a,4a-diaza-s-indacene-8-yl)-N-hexylbutanamide (13c). The synthesis followed the AMPS-DCT amide coupling procedure (section 5.1) using **13** as the carboxylic acid and hexylamine **c** as the amine. Fluorometer investigations into excitation and emission found 500 nm/511 nm ($\lambda_{max,abs}/\lambda_{max,em}$). MS (APCI) *m/z* calculated for $C_{23}H_{34}BF_2N_3O$ 417.3 found 417.4 (M), 403.2 (M - CH_3). ^{1}H NMR ($CDCl_3$, 500 MHz) δ 6.65 (s, 2H, pyrrole-H), 5.67 (s, 1H, -NH), 3.27 (t, 2H, -CH_2, *J* = 6.1 Hz), 2.98 (t, 2H, -CH_2, *J* = 6.1 Hz), 2.53 (s, 6H, -CH_3), 2.41 (t, 2H, -CH_2, *J* = 6.1 Hz), 2.30 (s, 6H, -CH_3), 2.09 (m, 2H, -CH_2), 1.45 (m, 2H, -CH_2), 1.32 (m, 2H, CH_2), 1.26 (m, 2H, -CH_2), 1.03 (t, 3H, -CH_3, *J* = 6.6 Hz); ^{13}C NMR ($CDCl_3$, 125 MHz) δ 177.8, 150.3, 146.2, 137.4, 131.3, 120.1, 43.9, 34.7, 31.2, 28.8, 26.7, 25.7, 23.5, 17.5, 15.6, 14.1, 12.9.

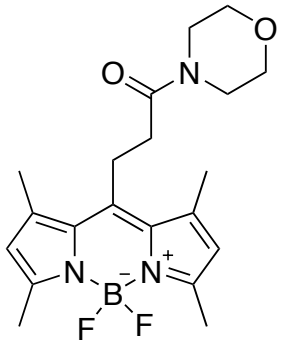

1-(Morpholin-4-yl)-3-(4,4-difluoro-1,3,5,7-tetramethyl-4-bora-3a,4a-diaza-s-indacene-8-yl)propan-1-one (16a). The synthesis followed the AMPS-DCT amide coupling procedure (section 5.1) using **16** as the carboxylic acid and morpholine **a** as the amine. Fluorometer investigations into excitation and emission found 501 nm/511 nm ($\lambda_{max,abs}/\lambda_{max,em}$). MS (APCI) *m/z* calculated for $C_{20}H_{26}BF_2N_3O_2$ 389.2 found 388.2 ($M - H^+$) and 375.6 ($M - CH_3$). ^{1}H NMR ($CDCl_3$, 500 MHz) δ 6.25 (s, 2H, pyrrole-H), 3.47 (m, 4H, $-CH_2$), 3.39 (m, 4H, $-CH_2$), 3.18 (t, 2H, $-CH_2$, J = 6.4 Hz), 2.82 (t, 2H, $-CH_2$, J = 6.4 Hz), 2.50 (s, 6H, $-CH_3$), 2.26 (s, 6H, $-CH_3$); ^{13}C NMR ($CDCl_3$, 125 MHz) δ 174.4, 153.1, 139.8, 137.4, 129.9, 120.6, 66.4, 43.1, 38.5, 20.1, 15.4, 14.1.

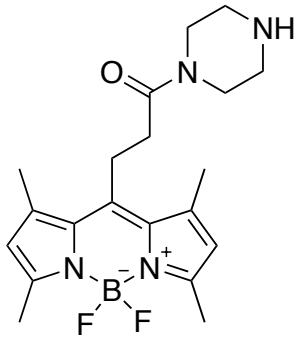

1-(piperazin-1-yl)-3-(4,4-Difluoro-1,3,5,7-tetramethyl-4-bora-3a,4a-diaza-s-indacene-8-yl)propan-1-one (16b). The synthesis followed the AMPS-DCT amide coupling procedure (section 5.1) using **16** as the carboxylic acid and piperazine **b** as the amine. Fluorometer investigations into excitation and emission found 501 nm/512 nm ($\lambda_{max,abs}/\lambda_{max,em}$). MS (APCI) *m/z* calculated for $C_{20}H_{27}BF_2N_4O$ 388.2 found 374.5 (M – CH_3), and 360.2 [M – $(CH_3)_2$]. ^{1}H NMR ($CDCl_3$, 500 MHz) δ 6.33 (s, 2H, pyrrole-H), 3.50 (m, 4H, -CH_2), 3.16 (t, 2H, -CH_2, *J* = 6.6 Hz), 2.85 (m, 4H, -CH_2), 2.62 (t, 2H, -CH_2, *J* = 6.6 Hz), 2.45 (s, 6H, -CH_3), 2.25 (s, 6H, -CH_3), 1.82 (s, 1H, -NH); ^{13}C NMR ($CDCl_3$, 125 MHz) δ 170.1, 155.9, 143.1, 142.3, 134.4, 123.5, 46.3, 44.9, 35.5, 21.7, 16.8, 13.9.

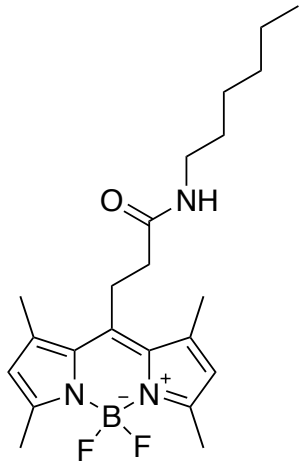

3-(4,4-Difluoro-1,3,5,7-tetramethyl-4-bora-3a,4a-diaza-s-indacene-8-yl)-N-hexylpropanamide (16c). The synthesis followed the AMPS-DCT amide coupling procedure (section 5.1) using **16** as the carboxylic acid and hexylamine **c** as the amine. Fluorometer investigations into excitation and emission found 503 nm/511 nm ($\lambda_{max,abs}/\lambda_{max,em}$). MS (APCI) *m/z* calculated for $C_{22}H_{32}BF_2N_3O$ 403.3 found 403.4 and 389.3 (M – CH_3). ^{1}H NMR ($CDCl_3$, 500 MHz) δ 6.39 (s, 2H, pyrrole-H), 5.63 (s, 1H, -NH), 3.35 (t, 2H, -CH_2, J = 6.6 Hz), 3.16 (t, 2H, -CH_2, J = 6.6 Hz), 2.77 (t, 2H, -CH_2, J = 6.6 Hz), 2.51 (s, 6H, -CH_3), 2.29 (s, 6H, -CH_3), 1.48 (m, 2H, -CH_2), 1.28 (m, 4H, -CH_2), 0.85 (t, 3H, -CH_3, J = 6.9 Hz); ^{13}C NMR ($CDCl_3$, 125 MHz) δ 174.2, 152.5, 149.1, 148.3, 133.8, 128.2, 39.3, 34.8, 31.0, 29.3, 28.7, 26.1, 22.1, 21.5, 15.2, 12.6.

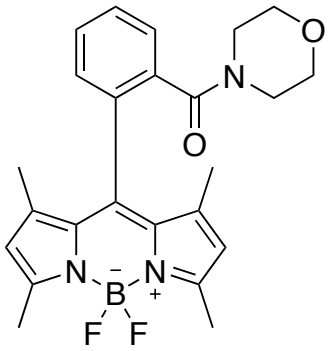

4-[2-(4,4-Difluoro-1,3,5,7-tetramethyl-4-bora-3a,4a-diaza-s-indacene-8-yl)benzoyl]morpholine (17a). The synthesis followed the AMPS-DCT amide coupling procedure (section 5.1) using **17** as the carboxylic acid and morpholine **a** as the amine. Fluorometer investigations into excitation and emission found 507nm/518nm ($\lambda_{max,abs}/\lambda_{max,em}$). MS (APCI) *m/z* calculated for $C_{24}H_{26}BF_2N_3O_2$ 437.2 found 437.3 and 417.9 ($M - F^-$). ^1H NMR ($CDCl_3$, 500 MHz) δ 8.03 (dd, J = 7.9 Hz, 1H), 7.55 (dd, J = 7.5 Hz, J = 2.2 Hz, 1H), 7.40 (dd, J = 7.5 Hz, J = 2.2 Hz, 1H), 7.24 (dd, J = 7.5 Hz, 1H), 6.26 (s, 2H, pyrrole-H), 3.63 (m, 4H, $-CH_2$), 3.51 (m, 4H, $-CH_2$), 2.51 (s, 6H, $-CH_3$), 2.28 (s, 6H, $-CH_3$); ^{13}C NMR ($CDCl_3$, 125 MHz) δ 170.2, 155.1, 151.2, 140.4, 135.9, 133.7, 130.0, 129.3, 128.5, 127.6, 126.9, 119.5, 67.1, 43.4, 14.1, 13.6.

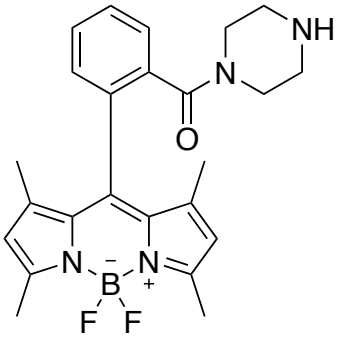

1-[2-(4,4-Difluoro-1,3,5,7-tetramethyl-4-bora-3a,4a-diaza-s-indacene-8-yl)benzoyl]piperazine (17b). The synthesis followed the AMPS-DCT amide coupling procedure (see section 5.1) using **17** as the carboxylic acid and piperazine **b** as the amine. Fluorometer investigations into excitation and emission found 505 nm/521 nm ($\lambda_{max,abs}/\lambda_{max,em}$). MS (APCI) *m/z* calculated for $C_{24}H_{27}BF_2N_4O$ 436.2 found 436.3 and 417.2 (M – F^-). ^{1}H NMR δ 7.92 (dd, *J* = 8.0 Hz, 1H), 7.68 (dd, *J* = 7.4 Hz, *J* = 2.0 Hz, 1H), 7.54 (dd, *J* = 7.4 Hz, *J* = 2.0 Hz, 1H), 7.42 (dd, *J* = 7.4 Hz, 1H), 6.13 (s, 2H, pyrrole-H), 3.42 (m, 4H, -CH_2), 2.94 (m, 4H, -CH_2), 2.32 (s, 6H, -CH_3), 2.21 (s, 6H, -CH_3), 1.92 (s, 1H, -NH); ^{13}C NMR ($CDCl_3$, 125 MHz) δ 167.7, 152.2, 143.1, 142.4, 135.2, 132.8, 130.7, 130.3, 129.9, 129.5, 129.1, 122.6, 48.0, 47.2, 13.1, 12.7.

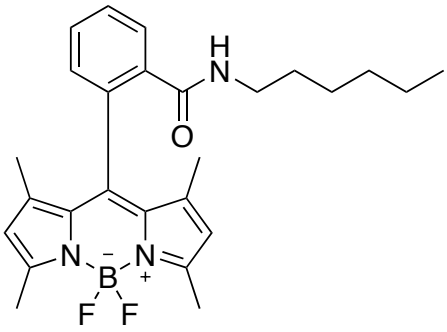

2-(4,4-Difluoro-1,3,5,7-tetramethyl-4-bora-3a,4a-diaza-s-indacene-8-yl)-N-hexylbenzamide (17c). This synthesis followed the AMPS-DCT amide coupling procedure (see section 5.1) using **17** as the carboxylic acid and hexylamine **c** as the amine. Fluorometer investigations into excitation and emission found 506 nm/517 nm ($\lambda_{max,abs}/\lambda_{max,em}$). MS (APCI) *m/z* calculated for $C_{26}H_{32}BF_2N_3O$ 451.3 found 432.3 ($M - F^-$).^{1}H NMR δ 8.35 (s, 1H, -NH), 7.87 (dd, *J* = 7.5 Hz, 1H), 7.55 (dd, *J* = 7.0 Hz, *J* = 2.0 Hz, 1H), 7.40 (dd, *J* = 7.0 Hz, *J* = 2.0 Hz, 1H), 7.29 (dd, *J* = 7.0 Hz, 1H), 6.23 (s, 2H, pyrrole-H), 3.30 (t, $-CH_2$, *J* = 6.2 Hz), 2.54 (s, 6H, $-CH_3$), 2.20 (s, 6H, $-CH_3$), 1.44 (m, 2H, $-CH_2$), 1.31 (m, 4H, $-CH_2$), 0.89 (t, 3H, $-CH_3$, *J* = 6.7 Hz); ^{13}C NMR ($CDCl_3$, 125 MHz) δ 169.3, 154.4, 151.2, 149.1, 140.6, 129.5, 129.1, 128.7, 127.6, 127.0, 126.3, 119.8, 40.1, 31.8, 29.5, 26.2, 22.0, 14.3, 13.0, 12.7.

6. REFERENCES

(1) Fu, Y.; Finney, N.S. *RSC Adv*. **2018**, 8(51), 29051-29061.
(2) Kaufman, T.S.; Ruveda, E.A. *Angew*. *Chem., Int. Ed.* **2005**, 44(6), 854-885.
(3) Teale, F.W.J.; Weber, G. *Biochem. J.* **2005**, 65(3), 476-482.
(4) Lavis, L.D.; Raines, R.T. *ACS Chem. Biol.* **2008**, 3(3), 142-155.
(5) Whitby, L.G. *Biochem. J.* **1953**, 54, 437-442.
(6) Hudson, E.N.; Weber, G. *Biochem. J.* **1973**, 12(21), 4154-4161.
(7) Meallier, P.; Guittonneau, S.; Emmelin, C.; Konstantinova, T. *Dyes Pigm.* **1999**, 40, 95-98.
(8) Brangato, R.; Bandello, F.; Lattanzio, R. *Surv. Ophthalmol*. **1997**, 42(1), 41-70.
(9) Steiner, M.; Gutbrodt, K.; Krall, N.; Neri, D. *Bioconjugate Chem*. **2013**, 24(2), 234-241.
(10) Liubchenko, G.A.; Moriev, R.M.; Kholodna, L.S. *Ukr. Biochem. J.* **2015**, 87, 33-45.
(11) Shcerbakova, D.M.; Subach, O.M.; Verkhusha, V.V. *Angew Chem. Int. Ed. Engl.* **2012**, 51(43), 10724-10738.
(12) Hell, S.W.; Wichmann, J. *Opt. Lett.* **1994**, 19(11), 780-782.
(13) Wang, L.; Frei, M.S.; Salim, A.; Johnsson, K. *J. Am. Chem. Soc.* **2019**, 141(7), 2770-2781.
(14) Zhang, X.; Chen, K.; Sun, W. *Chem. Eur. J.* **2020**, 27(16), 5107-5119.
(15) Lakowicz, J.R. Principles of Fluorescent Spectroscopy. *Springer*; 3rd ed. **2006**.
(16) Loudet, A.; Burgess, K. *Chem. Rev.* **2007**, 107(11), 4891-4932.
(17) Ulrich, G.; Ziessel, R.; Harriman, A. *Angew. Chem.* **2008**, 47(7), 1184-1201.
(18) Raveendran, A.V.; Sankeerthana, P.A.; Jayaraj, A.; Swamy, P.C.A. *Res. Chem.* **2022**, 4, 100297.
(19) Li, X.; Gao, Y.; James, T.D. *Chem. Comm.* **2012**, 48, 10121-10123.
(20) Hoye, A.T.; Davoren, P. *Acc. Chem. Res.* **2008**, 41, 87-97.
(21) Gao, T.; He, H.; Huang, R.; Zheng, M.; Wang, F.F.; Hu, Y.J.; Jiang, F.L.; Lu, Y. *Dyes Pigm.* **2017**, 141, 530-535.
(22) Gayathri, T.; Karnewar, S.; Kotamraju, S.; Singh, S.P. *ACS Med. Chem. Lett.* **2018**, 9(7), 618-622.
(23) Murale, D.P.; Haque, M.M.; Hong, S.C.; Jang, S.; Lee, J.H.; An, S.J.; Lee, J. *Dyes Pigm.* **2021**, 196, 109830.
(24) Sui, B.; Tang, S.; Woodward, A.W.; Kim, B.; Belfield, K.D. *Eur JOC*. **2016**, 16, 2851-2857.
(25) Metaxas A.; Kempf, S.J. *Neural Regen. Res.* **2016**, 11(10), 1579-1581.
(26) Soloperto, A., Quaglio, D., Baiocco, P., Romeo, I., Mori, M., Ardini, M., Presutti, C., Sannino, I., Ghirga, S., Iazzetti, A., Ippoliti, R., Ruocco, G.,

Botta, B., Ghirga, F., Angelantonio, S.D., Boffi, A. *Sci. Rep.* **2022**, 12, 5257.
(27) Li, Z.; Mintzer, E.; Bittman, R. *J. Org. Chem.* **2006**, 71(4), 1718-1721.
(28) Freiberg, K.M.; Kavthe, R.D.; Thomas, R.M.; Fialho, D.M.; Dee, P.; Scurria, M.; Lipshutz, B.H. *Chem. Sci.* **2023**, 14, 3462-3469.
(29) Wang, D.; Fan, J.; Gao, X.; Sun, S.; Peng, X. *J. Org. Chem.* **2009**, 74, 7675-7683.
(30) Ambroz, F.; Donnelly, J.L.; Wilden, J.D.; Macdonald, T.J; Parkin, I.P. *Nanomaterials (Basel)*. **2019**, 9(10), 1346.
(31) Nanda, J.S.; Lorsch, J.R. *Methods Enzymol.* **2014**, 536, 87-94.
(32) Ksenofontova, K.V., Kerner, A.A., Ksenofontov, A.A., Shagurin, A.Y., Bocharov, P.S., Lukanov, M.M., Kayumov, A., Zhuravleva, D., Iskhakova, Z., Molchanov, E., Merkushev, D., Khodov, I., Marfin, Y.S. *Molecules*. **2022**, 27(22), 7911.
(33) Sornay, C.; Vaur, V.; Wagner, A.; Chaubet, G. *R. Soc. Open Sci.* **2022**, 9(1), 211563.
(34) Klykov, O.; Weller, M.G. *Anal. Methods*. **2015**, 7, 6443-6448.
(35) Cankarova, N.; Schutznerova, E.; Krchnak, V. *Chem. Rev.* **2019**, 119(24), 12089-12207.
(36) Hwang, T.; Ranganathan, K.; Fang, Y.; Crockett, R.; Osgood, S.; Cui, S. *Org. Process Res. Dev.* **2018**, 22(8), 1007-1014.
(37) Liu, C.; Xie, J.; Wu, W.; Wang, M.; Chen, W.; Idres, S.B.; Rong, J.; Deng, L.; Khan, S.A.; Wu, J. *Nat. Chem.* **2021**, 13, 451-457.
(38) Coin, I.; Beyermann, M.; Bienert, M. *Nat. Protoc.* **2007**, 2, 3247-3256.
(39) Merrifield, R.B. *J. Am. Chem/ Soc.* **1963**, 85(14), 2149-2154.
(40) Boas, U.; Brask, J.; Jensen, K.J. *Chem. Rev.* **2009**, 109(5), 2092-2118.
(41) Fields, G.B.; Tian, Z.; Barany, G. In Synthetic Peptides, A User's Guide, 2nd ed.; Grant, G.A.; Ed.; W.H. Freeman and Company: New York, **2002**, pp 93-219.
(42) Crosignani, S.; White, P.D.; Steinauer, R.; Linclau, B. *Org. Lett.* **2003**, 5(6), 853-856.
(43) Kumar, M.K.; Mathew, B.M. *Protein Pept. Lett.* **2002**, 9(2), 167-172.
(44) Holte, P.; Wijgergangs, J.; Thijs, L.; Zwanenburg, B. *Org. Lett.* **1999**, 1(7), 1095-1097.
(45) Zhao, Y.; Pirrung, M.C.; Liao, J. *Mol. Biosyst.* **2012**, 8(3), 879-887.
(46) Krajcovicova, S.; Stankova, J.; Dzubak, P.; Hajduch, M.; Soural, M.; Urban, M. *Chem. Eur. J.* **2018**, 24, 4957-4966.
(47) Harris, P.; Yang, S.H.; Brimble, M.A. *Tetrahedron Lett.* **2011**, 52(45), 6024-6026.
(48) Flon, V.; Benard, M.; Schapman, D.; Galas, L.; Renard, P.; Sabot, C. *Biomolecules*. **2020**, 10(4), 619.
(49) Zhou, Y.; Liang, X. *RSC Adv*. **2021**, 11(60), 37942-37951.
(50) Abdildinova, A.; Kurth, M.J.; Gong, Y. *Pharmaceuticals*. **2021**, 14(5), 449.
(51) Mandaric, B. Personal communication, Lakehead University.

(52) Suna, G., Erdemir, E., Gunduz, S., Ozturk, T., Karakus, E. *ACS Omega*. **2023**, 8(25), 22984-22991.
(53) Gallegos, M., Costales, A., Pendas, A.M. *J. Comput. Chem.* **2022**, 43(11), 785-795.
(54) Cao, Q., Nicholson, W.I., Jones, A.C., Browne, D.L. *Org. Biomol. Chem.* **2019**, 17, 1722-1726.
(55) Riwar, L., Trapp, N., Kuhn, B., Diederich, F. *Angew. Chem. Int. Ed.* **2017**, 56(37), 11252-11257.
(56) Walter, E., Lee, L., Leung, P., Lo, K., Long, N. *Chem. Sci.* **2024**, 15, 4846-4852.
(57) Bassan, E., Gualandi, A., Cozzi, P., Ceroni, P. *Chem. Sci.* **2021**, 12, 6607-6628.
(58) Banuelos, J., Arroyo-Cordoba, I., Valois-Escamilla, I., Alvarez-Hernandez, A., Pena-Cabrera, E., Hu, R., Tang, B., Esnal, I., Martinez, V., Arbeloa, I. *RSC Adv.* **2011**, 1, 677-684.